Electronic Supplementary Information

Complexation of pentiptycene-derived trans-bis(crown ether) host with different terminal functional paraquat derivatives in solution and solid state: a switchable complexation process controlled by potassium ions

Ying-Xian Ma,[a,b] Ying Han,[a] Jing Cao[a] and Chuan-Feng Chen[*,a]

[a]Beijing National Laboratory for Molecular Sciences, CAS Key Laboratory of Molecular Recognition and Function, Institute of Chemistry, Chinese Academy of Sciences, Beijing 100190, China. [b]University of Chinese Academy of Sciences, Beijing 100049, China.

E-mail: cchen@iccas.ac.cn

Contents

1. Comparison of partial ^{1}H NMR spectra between the host and the guests

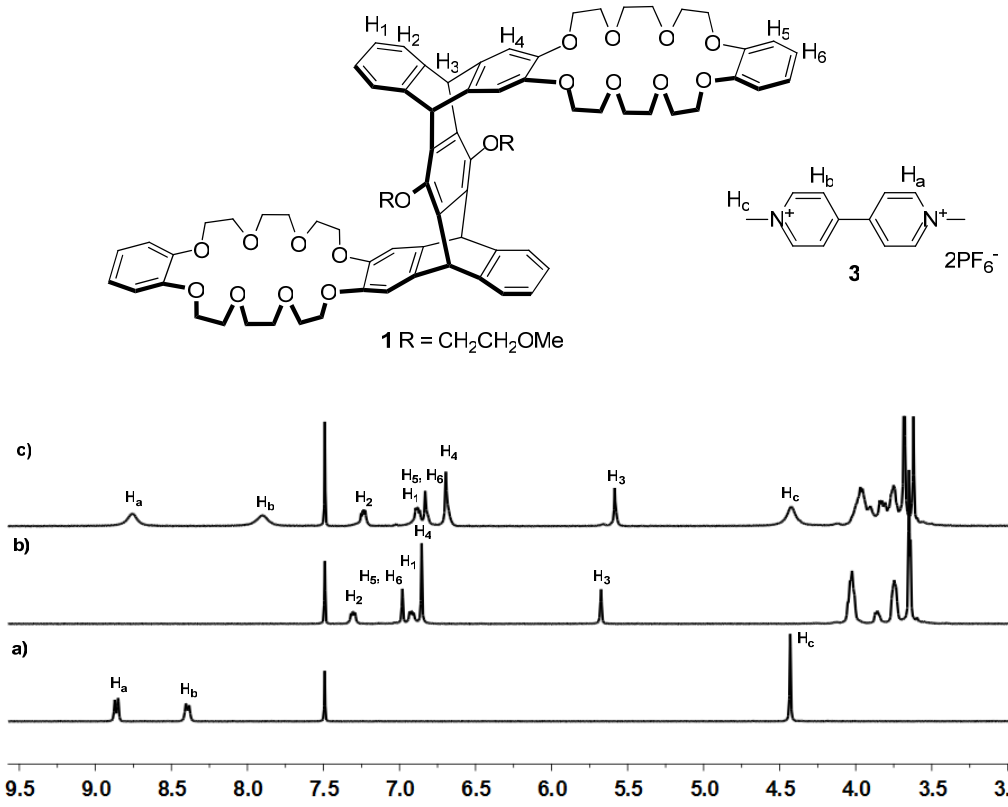

Fig. S1 Partial ^{1}H NMR spectra (300 MHz, $CD_3CN/CDCl_3$=1:1, v/v, 295K) of (a) free guest **3**, (b) free host **1**, and (c) **1** and 2.0 equiv. of **3**. $[\mathbf{1}]_0$=3.0 mM.

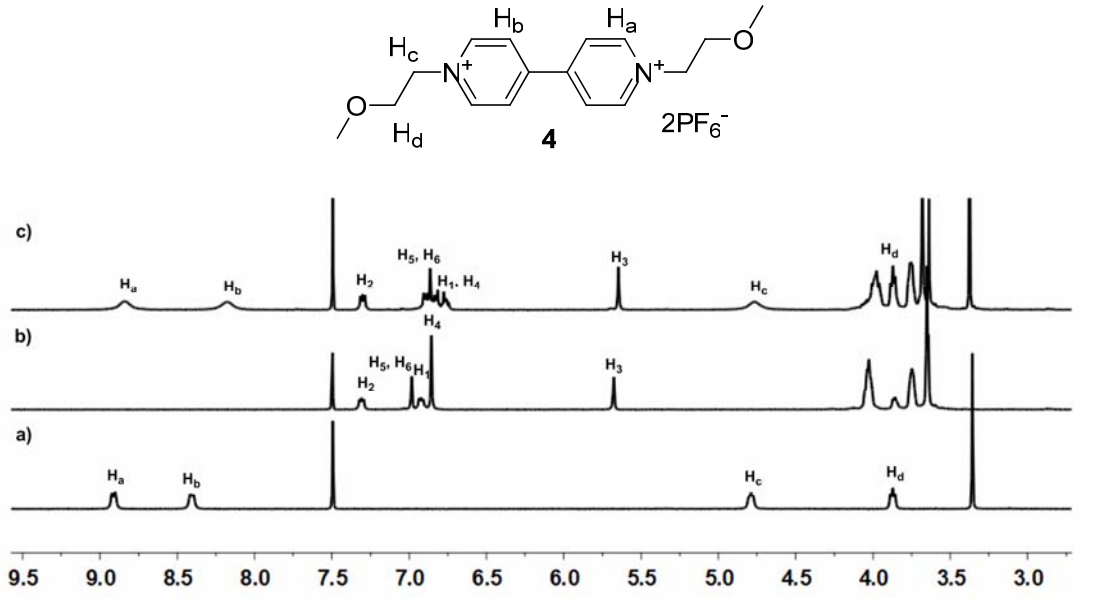

Fig. S2 Partial ^{1}H NMR spectra (300 MHz, $CD_3CN/CDCl_3$=1:1, v/v, 295K) of (a) free guest **4**, (b) free host **1**, and (c) **1** and 2.0 equiv. of **4**. $[\mathbf{1}]_0$=3.0 mM.

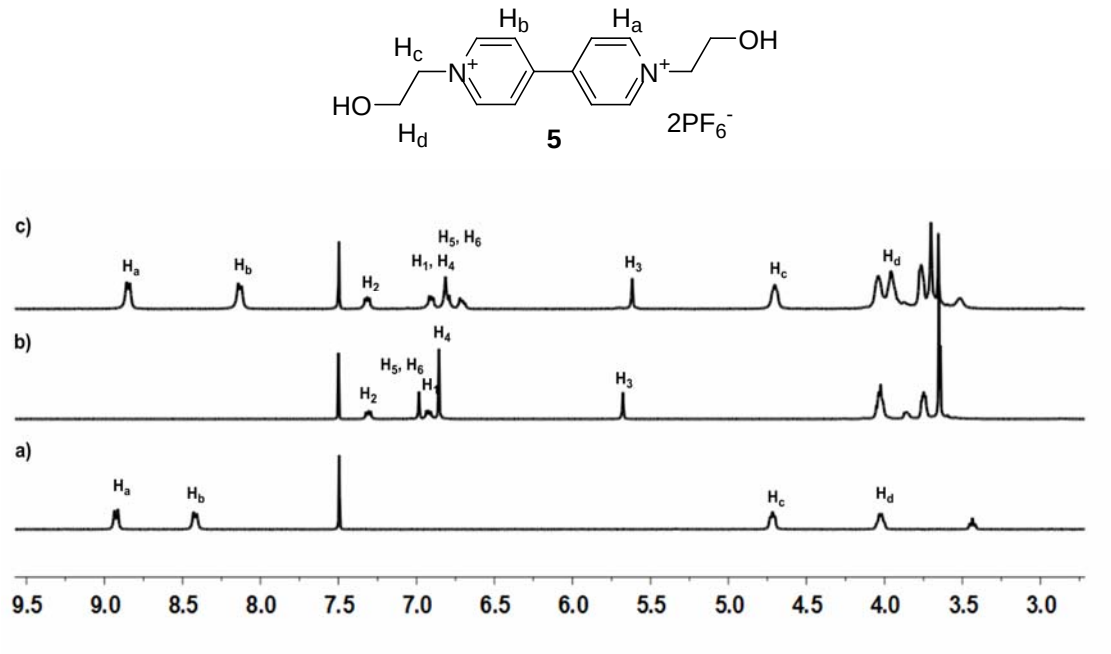

Fig. S3 Partial ^{1}H NMR spectra (300 MHz, $CD_3CN/CDCl_3$=1:1, v/v, 295K) of (a) free guest **5**, (b) free host **1**, and (c) **1** and 2.0 equiv. of **5**. $[\mathbf{1}]_0$=3.0 mM.

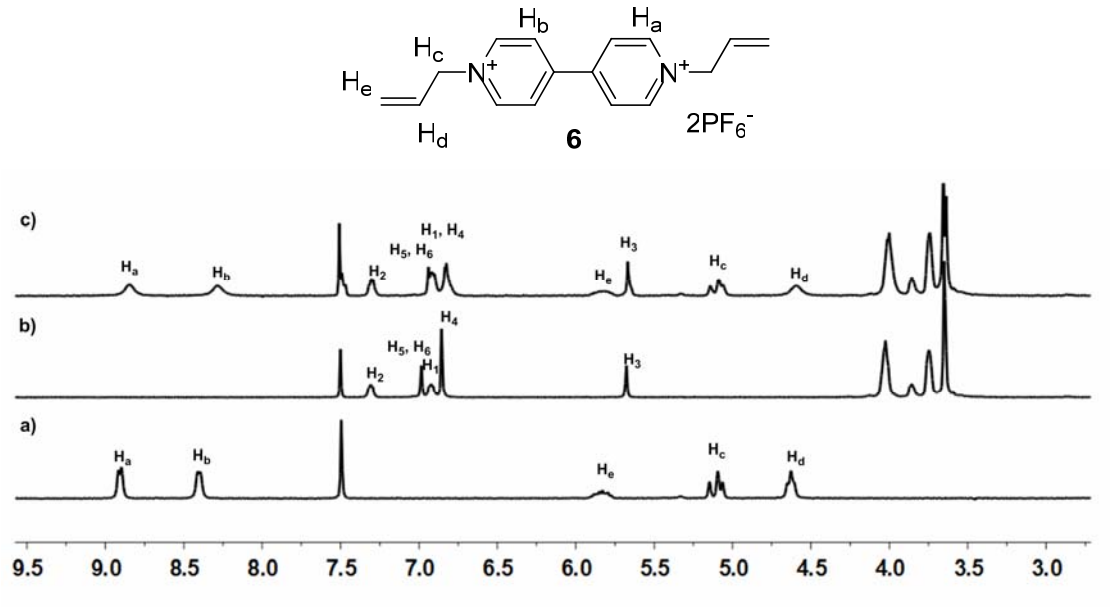

Fig. S4 Partial ^{1}H NMR spectra (300 MHz, $CD_3CN/CDCl_3$=1:1, v/v, 295K) of (a) free guest **6**, (b) free host **1**, and (c) **1** and 2.0 equiv. of **6**. $[\mathbf{1}]_0$=3.0 mM.

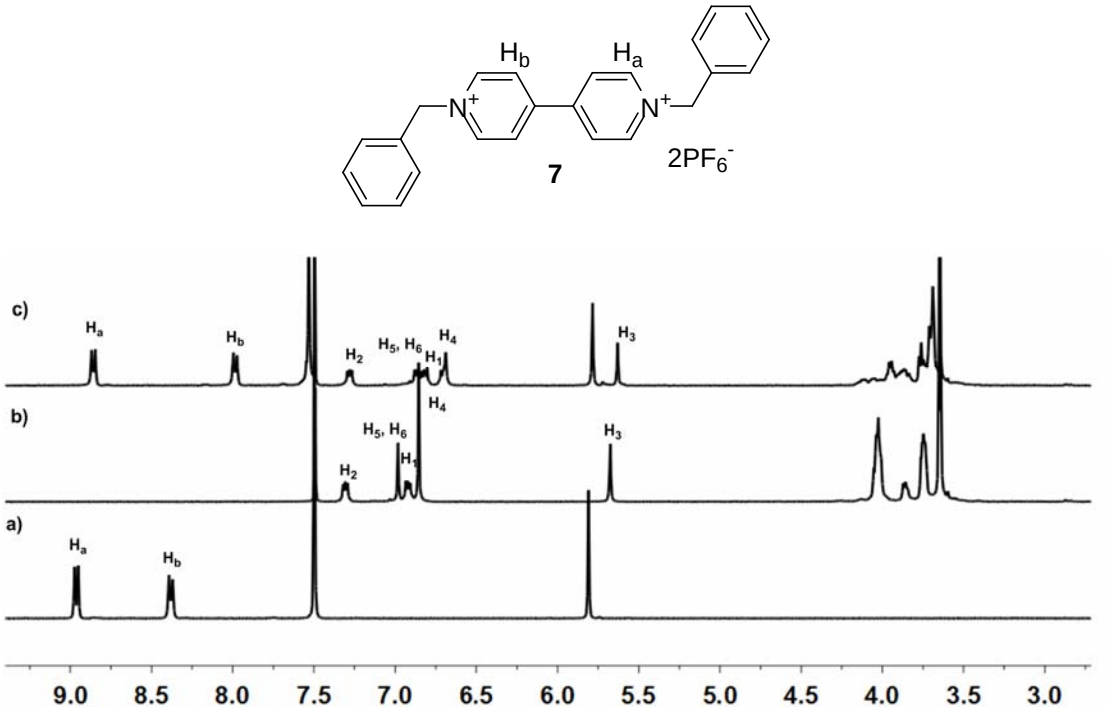

Fig. S5 Partial ^{1}H NMR spectra (300 MHz, $CD_3CN/CDCl_3$=1:1, v/v, 295K) of (a) free guest **7**, (b) free host **1**, and (c) **1** and 2.0 equiv. of **7**. $[\mathbf{1}]_0$=3.0 mM.

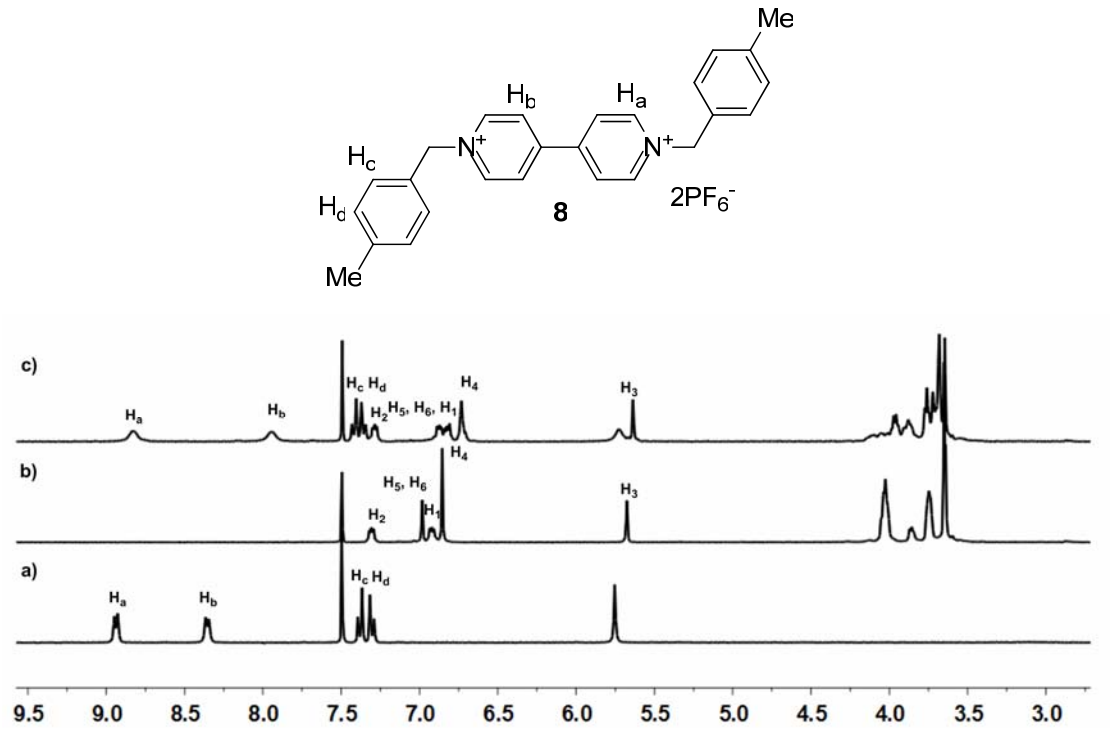

Fig. S6 Partial ^{1}H NMR spectra (300 MHz, $CD_3CN/CDCl_3$=1:1, v/v, 295K) of (a) free guest **8**, (b) free host **1**, and (c) **1** and 2.0 equiv. of **8**. $[\mathbf{1}]_0$=3.0 mM.

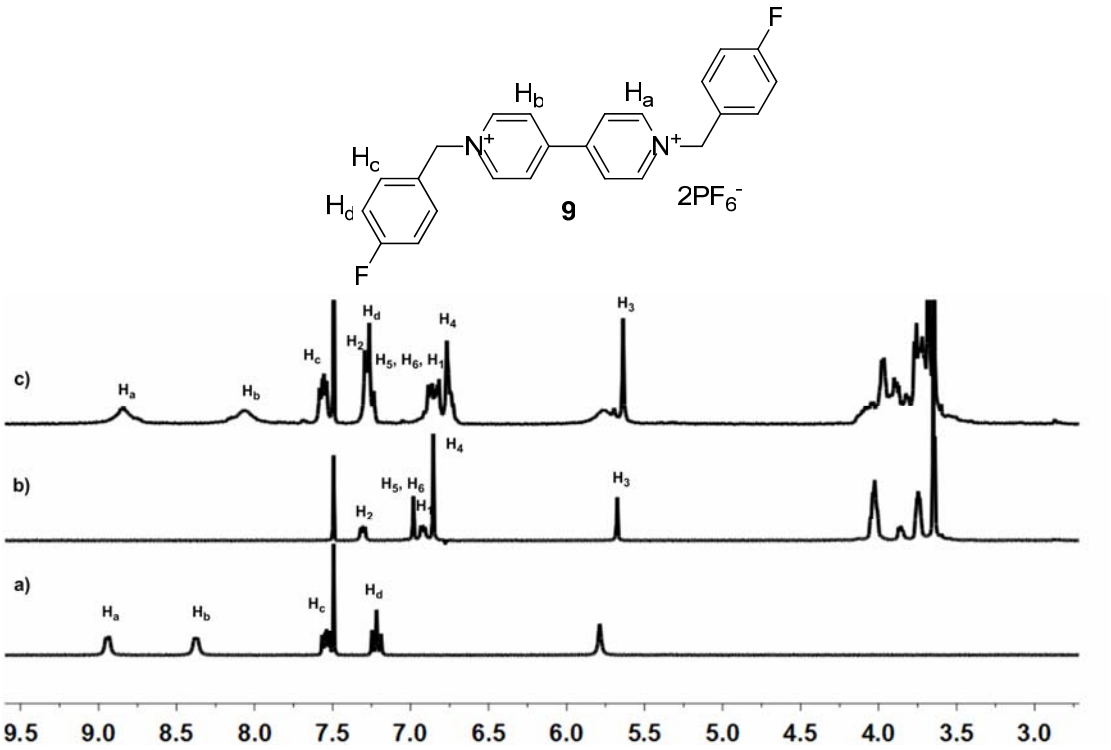

Fig. S7 Partial ^{1}H NMR spectra (300 MHz, $CD_3CN/CDCl_3$=1:1, v/v, 295K) of (a) free guest **9**, (b) free host **1**, and (c) **1** and 2.0 equiv. of **9**. $[\mathbf{1}]_0$=3.0 mM.

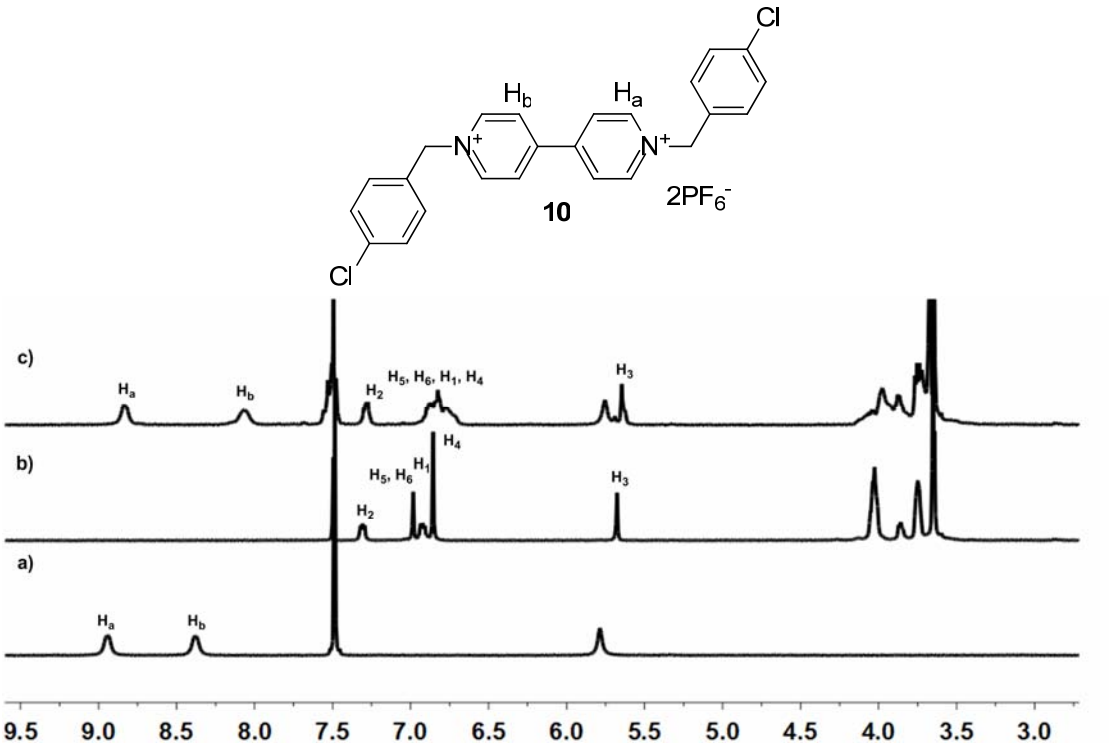

Fig. S8 Partial ^{1}H NMR spectra (300 MHz, $CD_3CN/CDCl_3$=1:1, v/v, 295K) of (a) free guest **10**, (b) free host **1**, and (c) **1** and 2.0 equiv. of **10**. $[\mathbf{1}]_0$=3.0 mM.

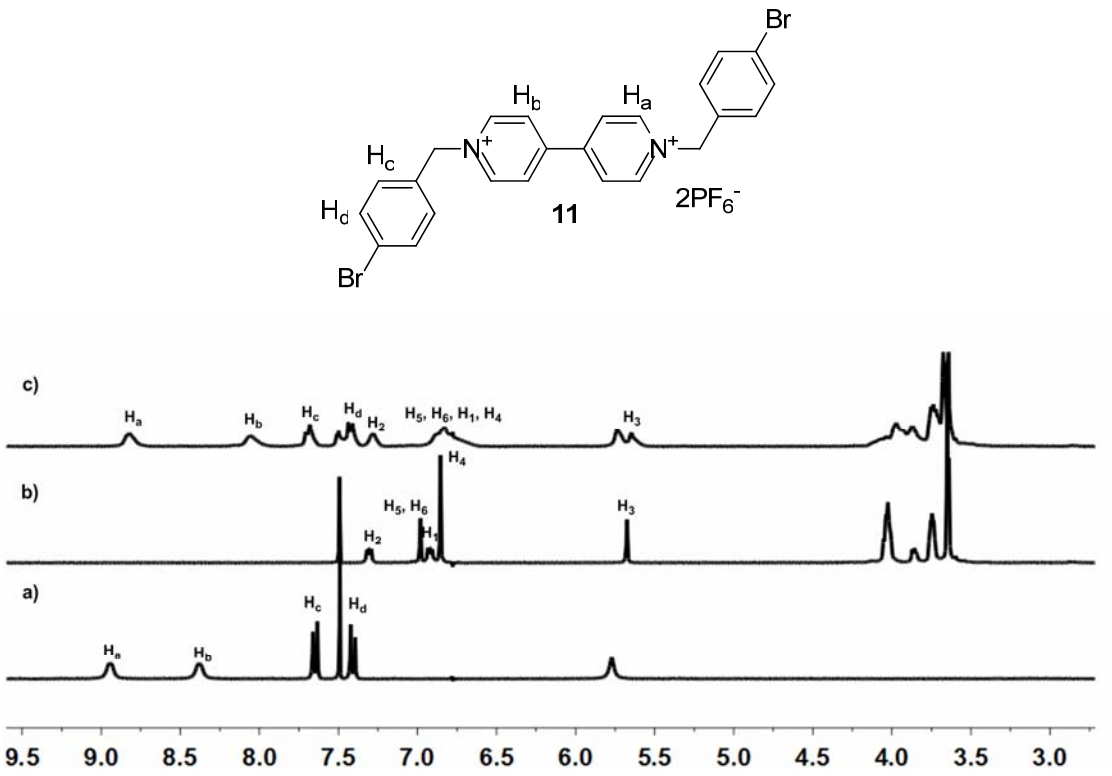

Fig. S9 Partial ^{1}H NMR spectra (300 MHz, $CD_3CN/CDCl_3$=1:1, v/v, 295K) of (a) free guest **11**, (b) free host **1**, and (c) **1** and 2.0 equiv. of **11**. $[\mathbf{1}]_0$=3.0 mM.

2. Determination of the association constants of complexes

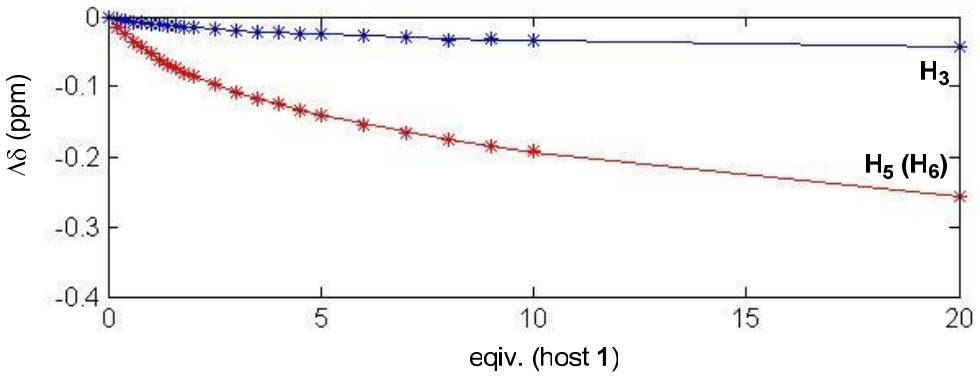

Fig. S10 Plot of ^{1}H NMR signal shifts observed in the titration of guest **2** with host **1**.

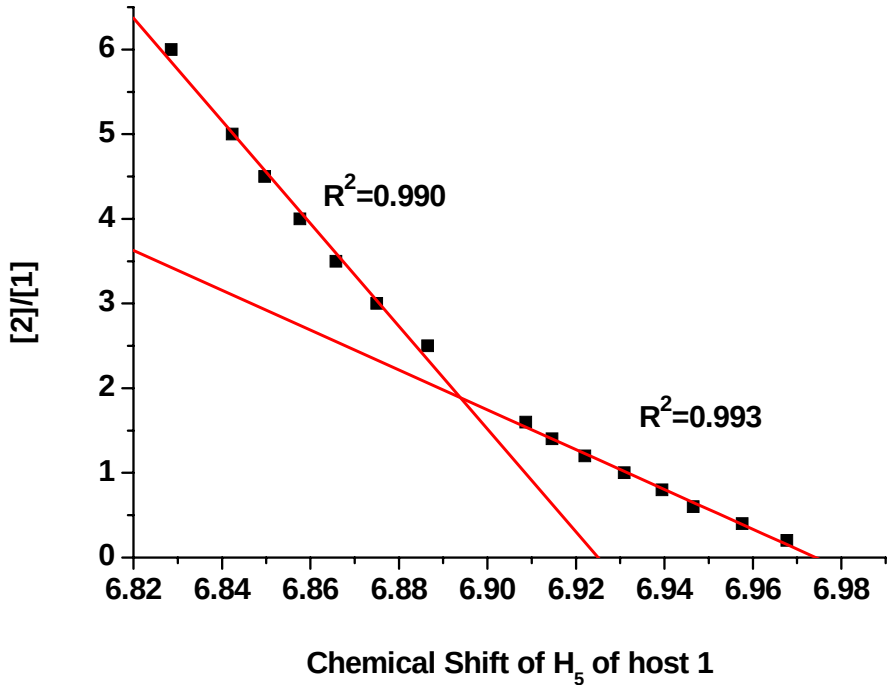

Fig. S11 Mole ratio plot for the complexation of **1** and **2** in $CD_3CN/CDCl_3$ = 1:1 at 298 K.

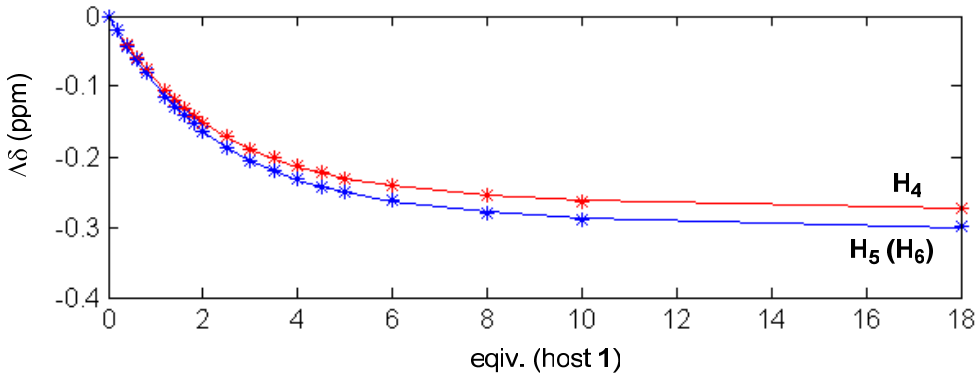

Fig. S12 Plot of ^{1}H NMR signal shifts observed in the titration of guest **3** with host **1**.

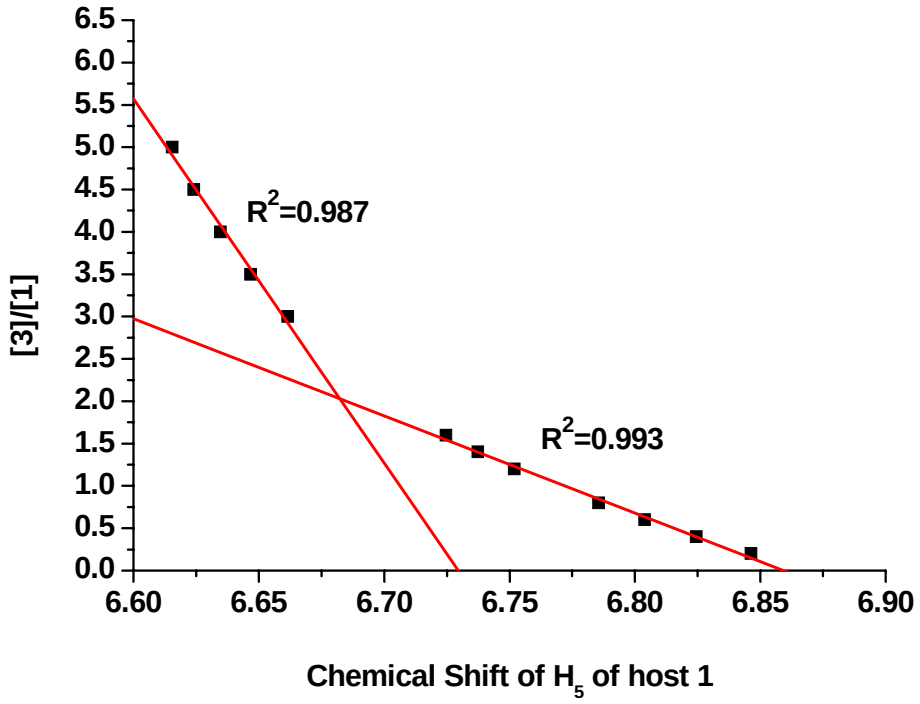

Fig. S13 Mole ratio plot for the complexation of **1** and **3** in $CD_3CN/CDCl_3$ = 1:1 at 298 K.

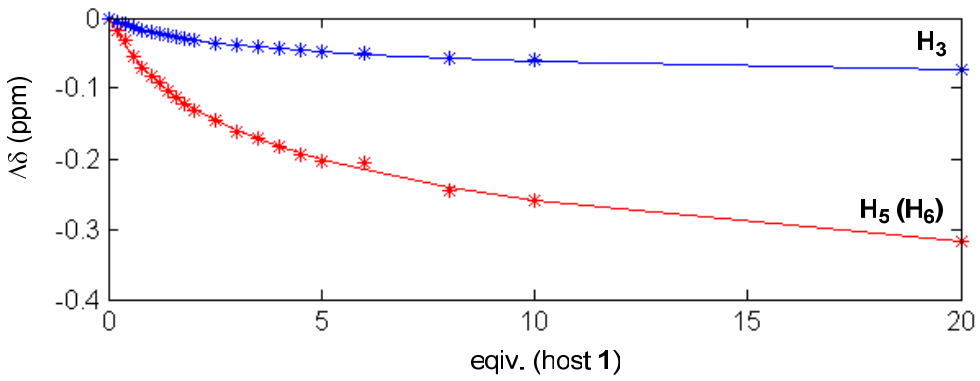

Fig. S14 Plot of ^{1}H NMR signal shifts observed in the titration of guest **4** with host **1**.

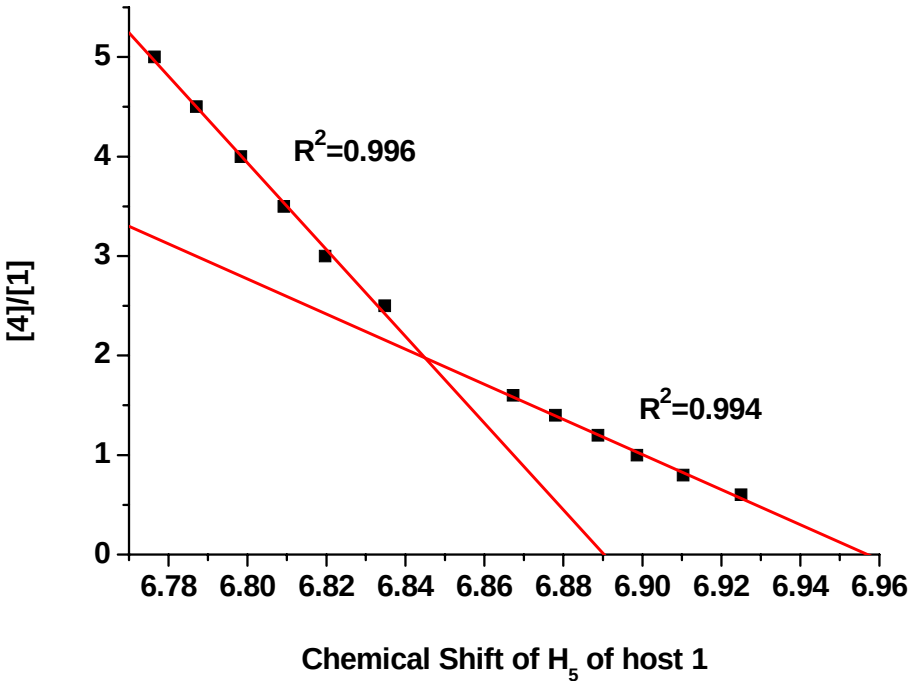

Fig. S15 Mole ratio plot for the complexation of **1** and **4** in $CD_3CN/CDCl_3$ = 1:1 at 298 K.

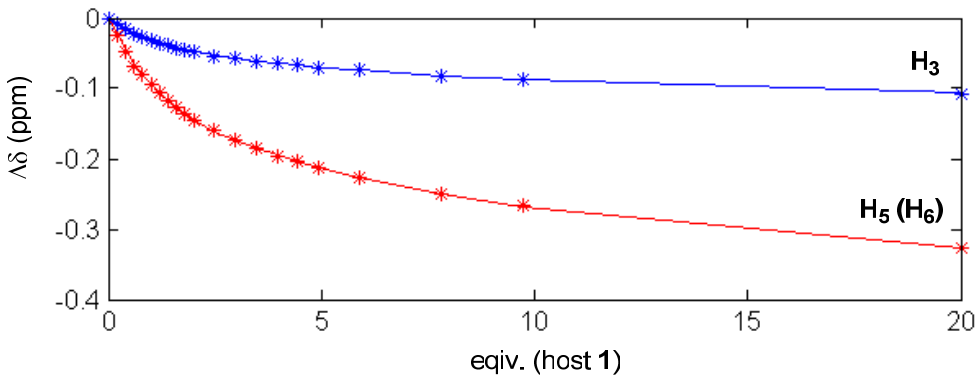

Fig. S16 Plot of ^{1}H NMR signal shifts observed in the titration of guest **5** with host **1**.

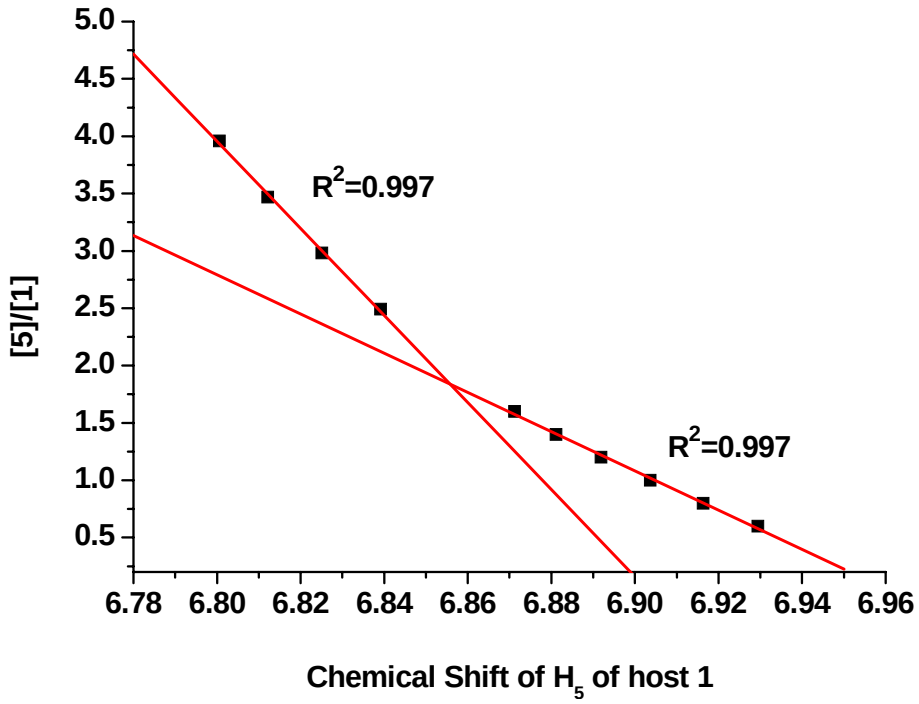

Fig. S17 Mole ratio plot for the complexation of **1** and **5** in $CD_3CN/CDCl_3$ = 1:1 at 298 K.

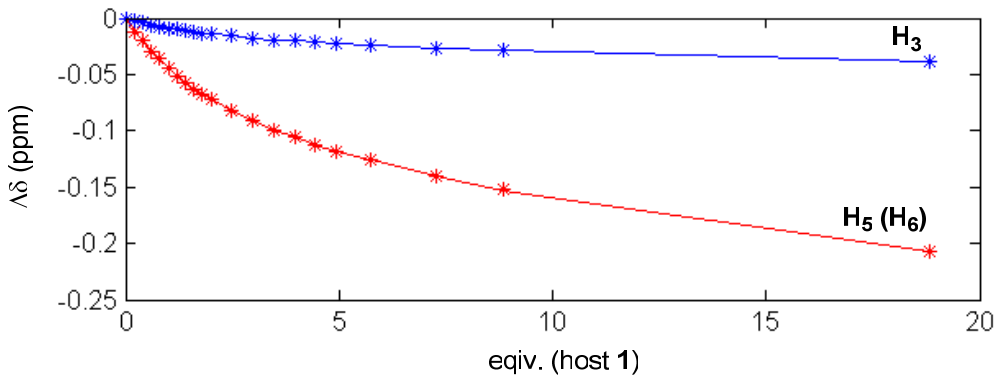

Fig. S16 Plot of ^{1}H NMR signal shifts observed in the titration of guest **6** with host **1**.

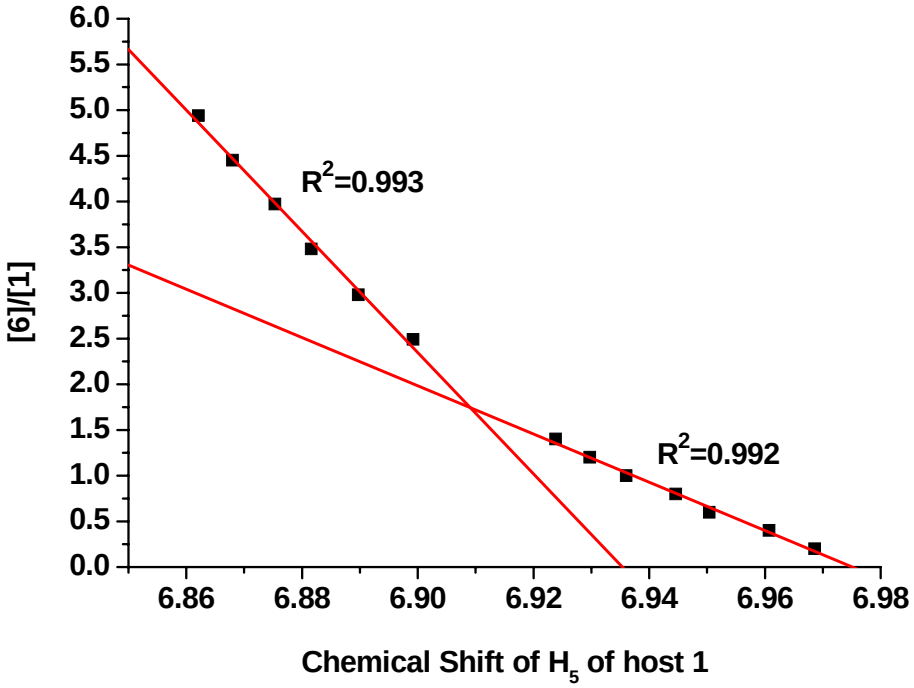

Fig. S17 Mole ratio plot for the complexation of **1** and **6** in $CD_3CN/CDCl_3$ = 1:1 at 298 K.

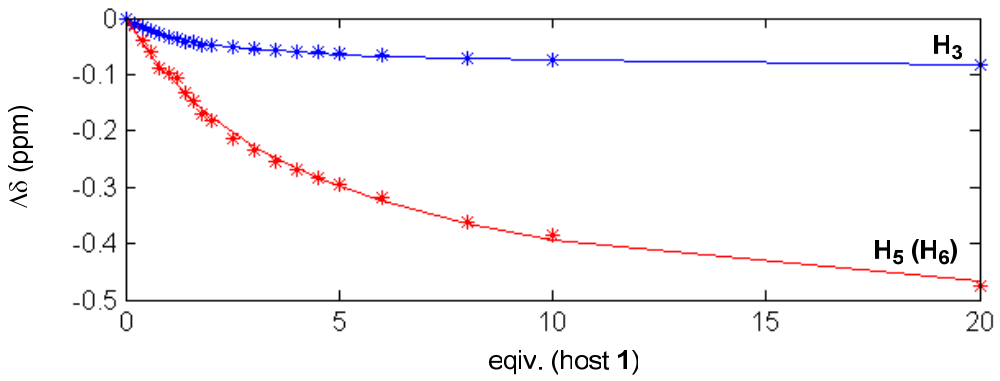

Fig. S18 Plot of ^{1}H NMR signal shifts observed in the titration of guest **7** with host **1**.

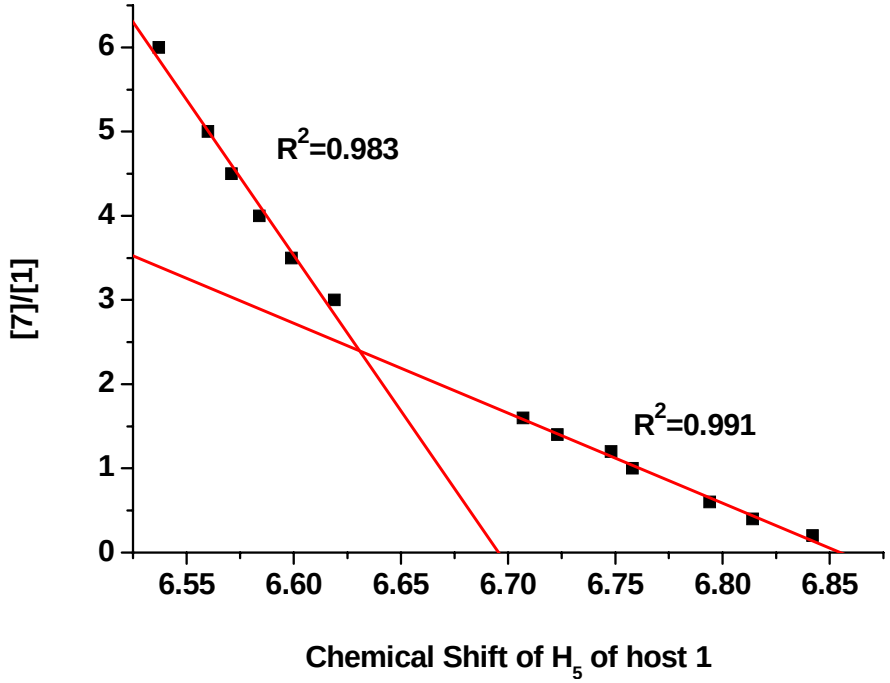

Fig. S19 Mole ratio plot for the complexation of **1** and **7** in $CD_3CN/CDCl_3$ = 1:1 at 298 K.

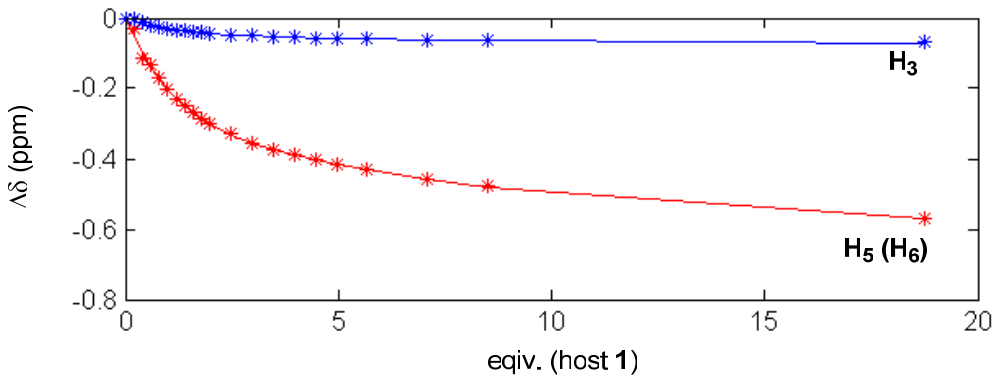

Fig. S20 Plot of ^{1}H NMR signal shifts observed in the titration of guest **8** with host **1**.

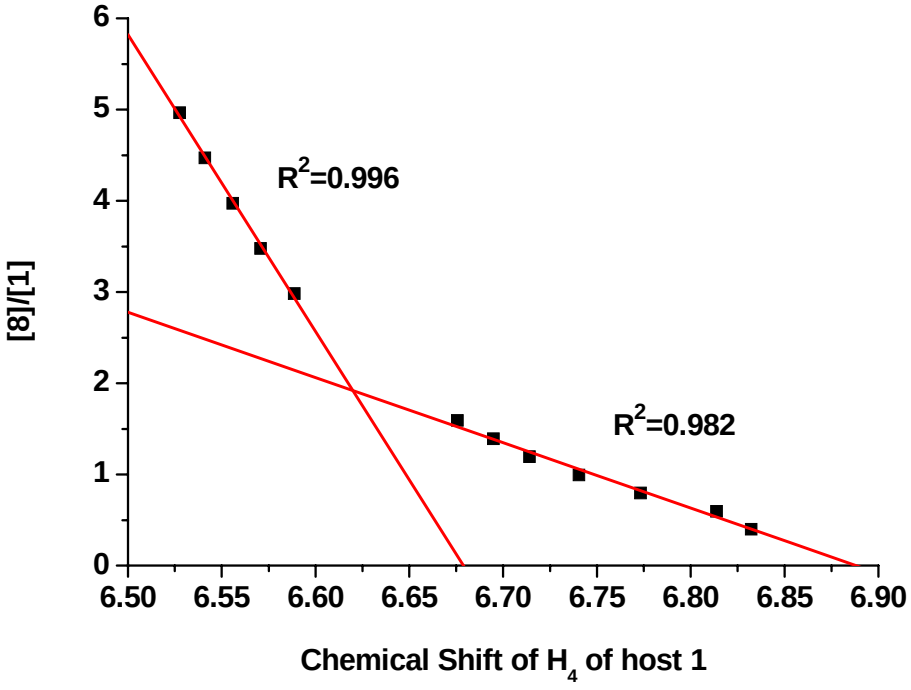

Fig. S21 Mole ratio plot for the complexation of **1** and **8** in $CD_3CN/CDCl_3$ = 1:1 at 298 K.

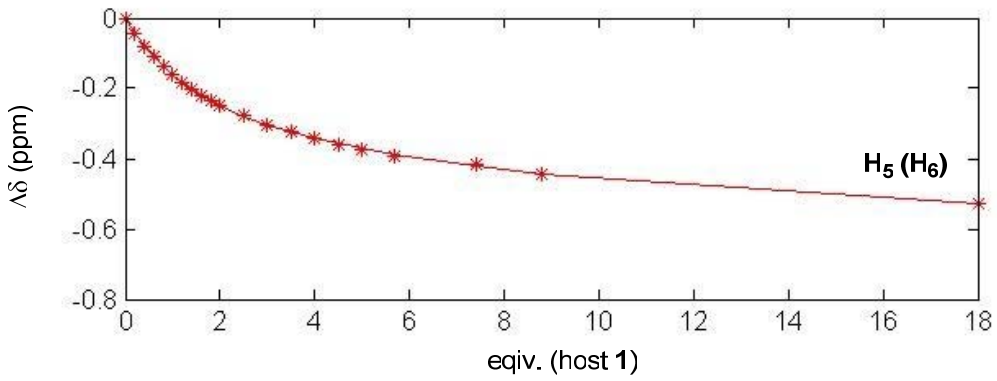

Fig. S22 Plot of ^{1}H NMR signal shifts observed in the titration of guest **9** with host **1**.

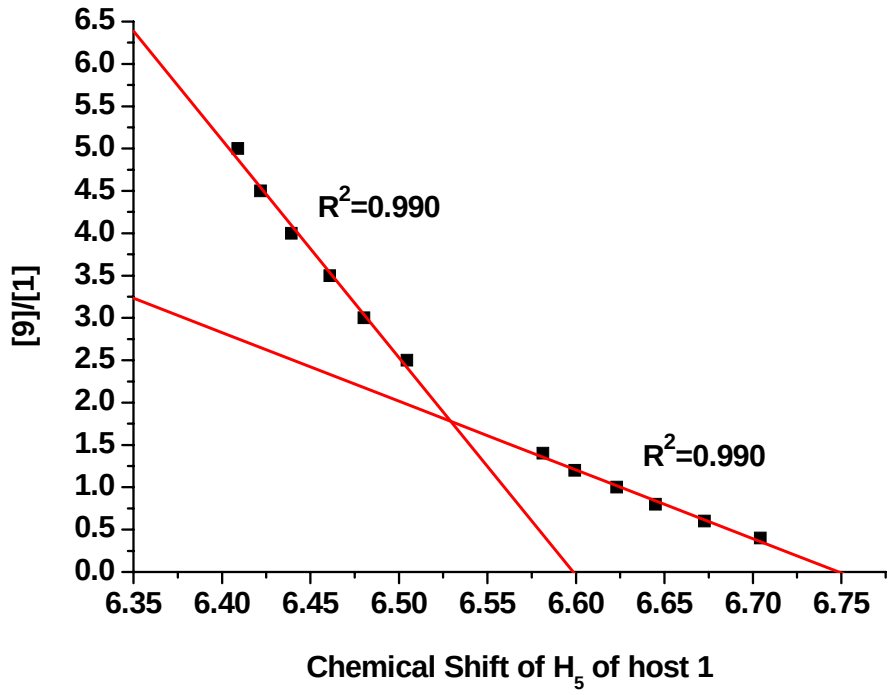

Fig. S23 Mole ratio plot for the complexation of **1** and **9** in $CD_3CN/CDCl_3$ = 1:1 at 298 K.

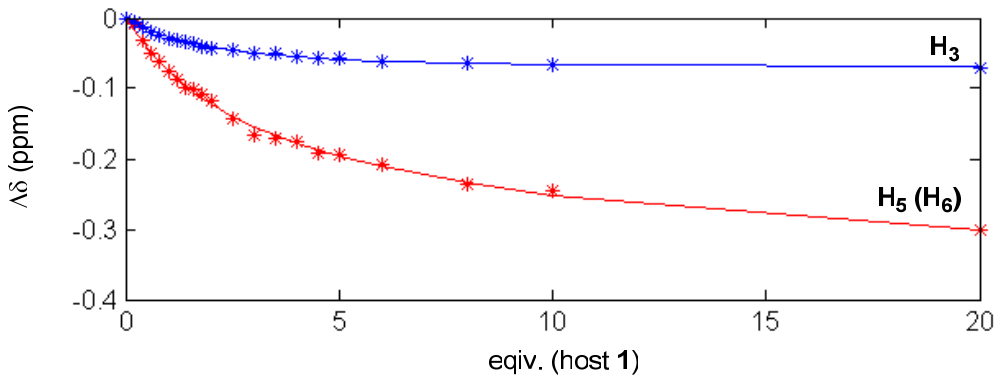

Fig. S24 Plot of ^{1}H NMR signal shifts observed in the titration of guest **10** with host **1**.

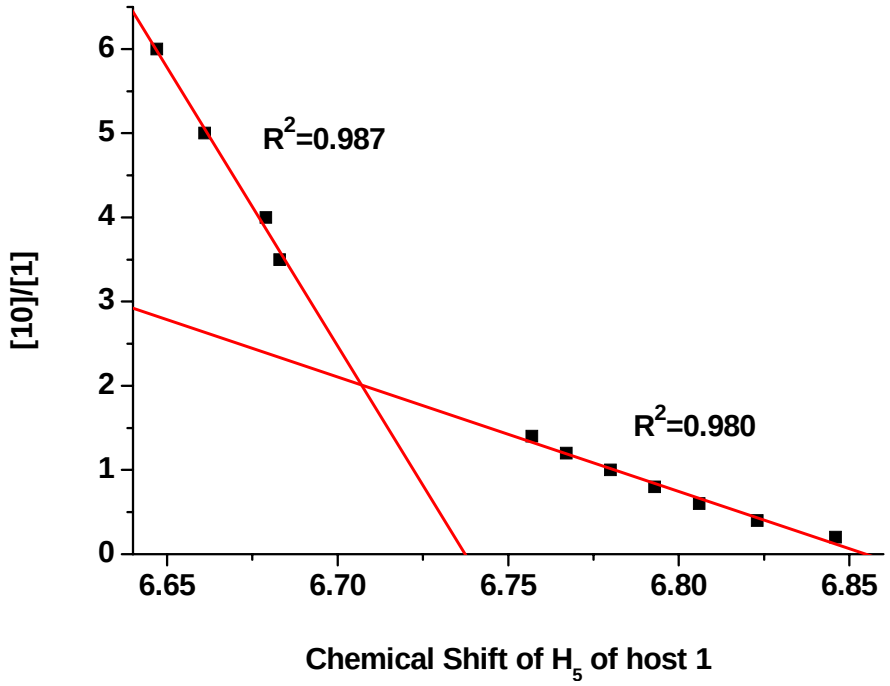

Fig. S25 Mole ratio plot for the complexation of **1** and **10** in $CD_3CN/CDCl_3$ = 1:1 at 298 K.

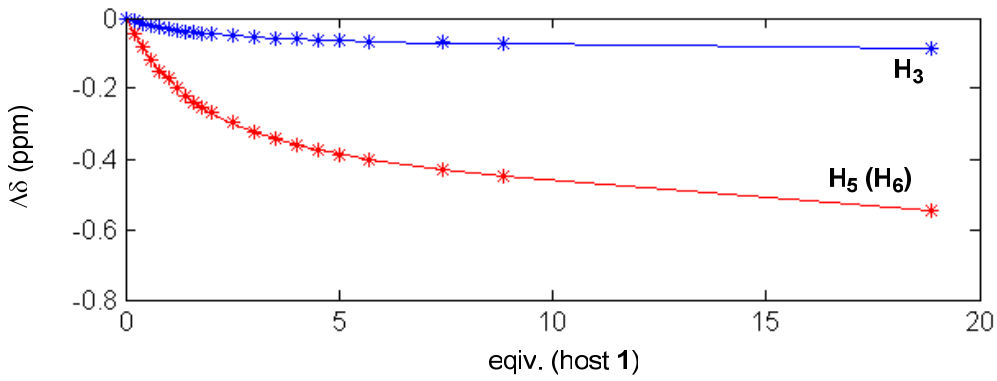

Fig. S26 Plot of ^{1}H NMR signal shifts observed in the titration of guest **11** with host **1**.

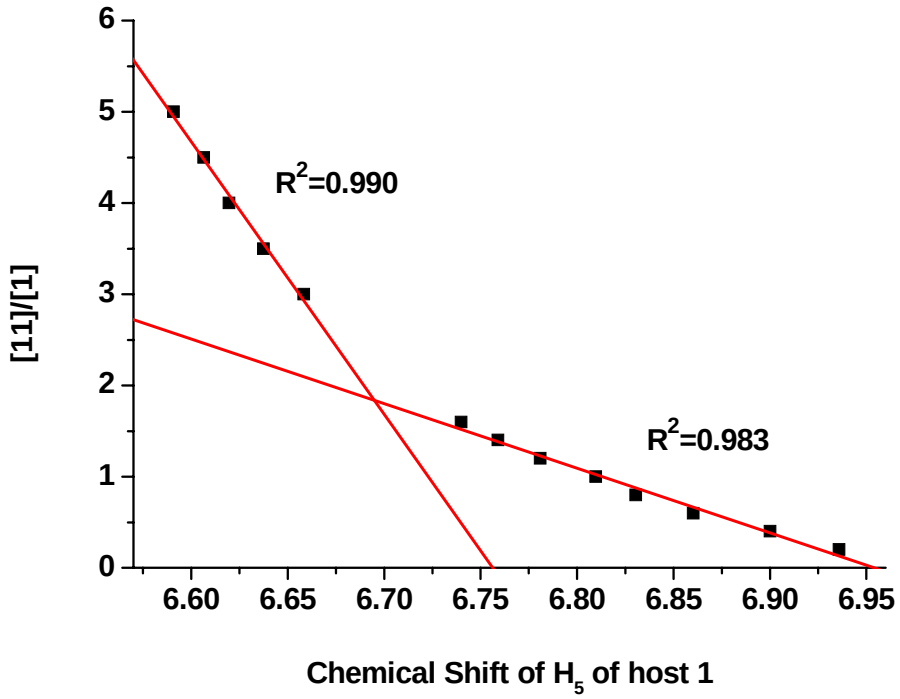

Fig. S27 Mole ratio plot for the complexation of **1** and **11** in $CD_3CN/CDCl_3$ = 1:1 at 298 K.

3. Comparison of ^{1}H NMR spectra by the removal and addition of the K^+ ions

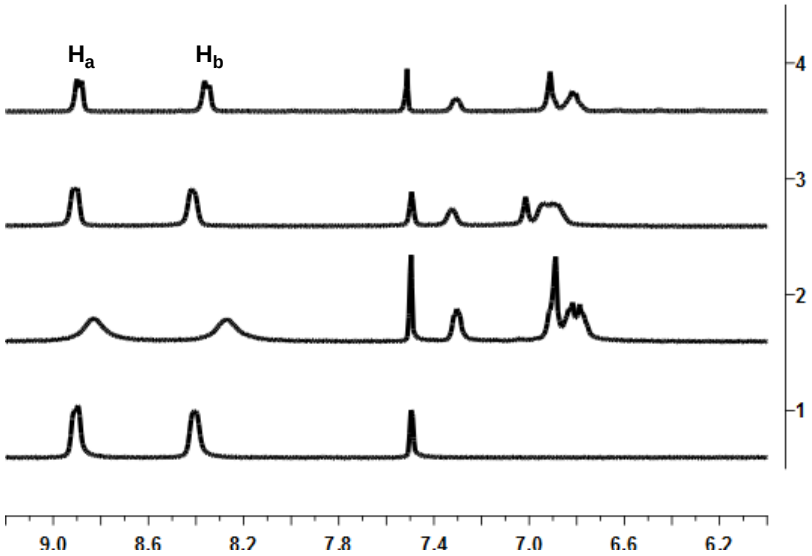

Fig. S28 Partial ^{1}H NMR spectra (300 MHz, $CD_3CN/CDCl_3$= 1:1, v/v, 298K) of (1) free **2**, (2) **1** and 2.0 equiv. of **2**, (3) to the solution of 2 was added 4.0 equiv. of KPF_6, and (4) to the solution of 3 was added 6.0 equiv. of [18]-crown-6. $[\mathbf{1}]_0$ = 3.0 mM.

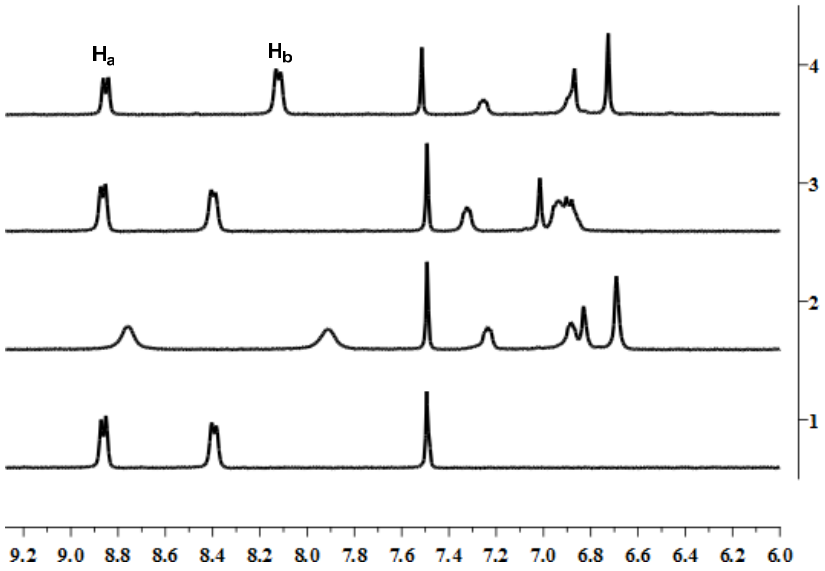

Fig. S29 Partial ^{1}H NMR spectra (300 MHz, $CD_3CN/CDCl_3$= 1:1, v/v, 298K) of (1) free **3**, (2) **1** and 2.0 equiv. of **3**, (3) to the solution of 2 was added 4.0 equiv. of KPF_6, and (4) to the solution of 3 was added 6.0 equiv. of [18]-crown-6. $[\mathbf{1}]_0$ = 3.0 mM.

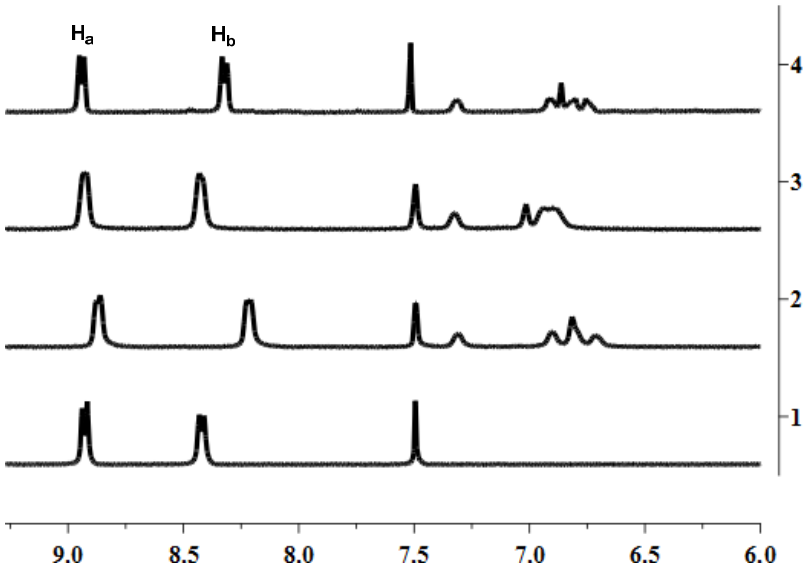

Fig. S30 Partial ^{1}H NMR spectra (300 MHz, $CD_3CN/CDCl_3$= 1:1, v/v, 298K) of (1) free **5**, (2) **1** and 2.0 equiv. of **5**, (3) to the solution of 2 was added 4.0 equiv. of KPF_6, and (4) to the solution of 3 was added 6.0 equiv. of [18]-crown-6. $[\mathbf{1}]_0$ = 3.0 mM.

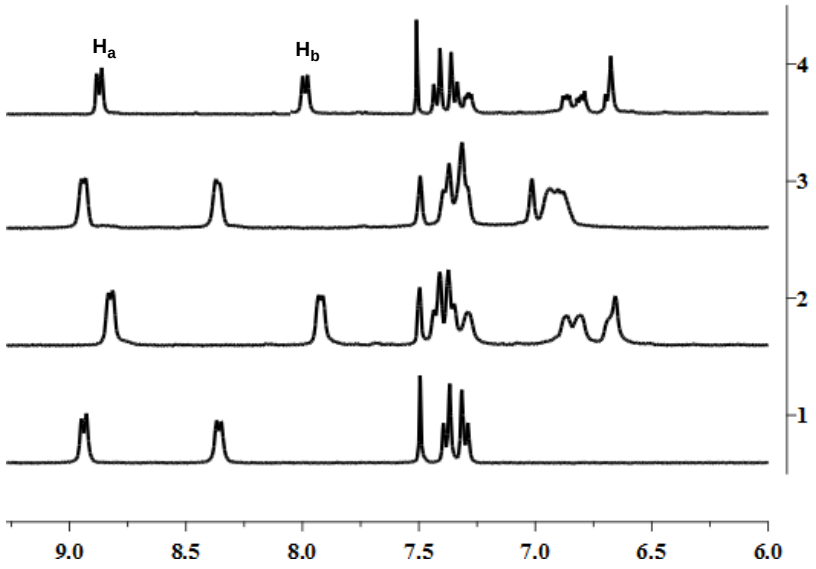

Fig. S31 Partial ^{1}H NMR spectra (300 MHz, $CD_3CN/CDCl_3$= 1:1, v/v, 298K) of (1) free **8**, (2) **1** and 2.0 equiv. of **8**, (3) to the solution of 2 was added 4.0 equiv. of KPF_6, and (4) to the solution of 3 was added 6.0 equiv. of [18]-crown-6. $[\mathbf{1}]_0$ = 3.0 mM.

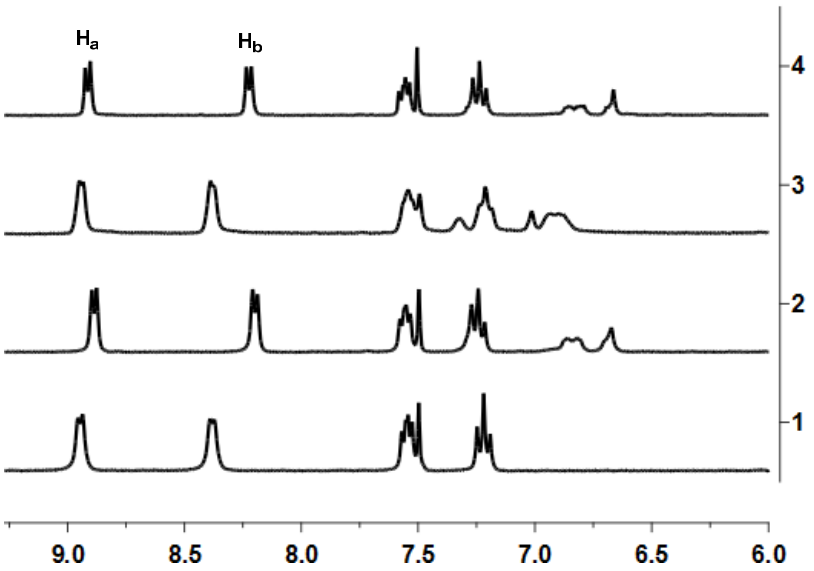

Fig. S32 Partial ^{1}H NMR spectra (300 MHz, $CD_3CN/CDCl_3$= 1:1, v/v, 298K) of (1) free **9**, (2) **1** and 2.0 equiv. of **9**, (3) to the solution of 2 was added 4.0 equiv. of KPF_6, and (4) to the solution of 3 was added 6.0 equiv. of [18]-crown-6. $[\mathbf{1}]_0$ = 3.0 mM.

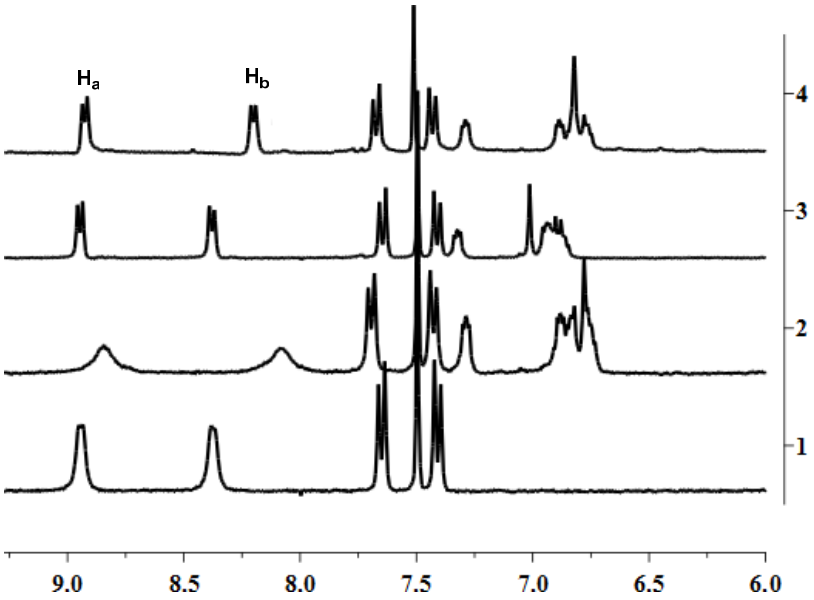

Fig. S33 Partial ^{1}H NMR spectra (300 MHz, $CD_3CN/CDCl_3$= 1:1, v/v, 298K) of (1) free **11**, (2) **1** and 2.0 equiv. of **11**, (3) to the solution of 2 was added 4.0 equiv. of KPF_6, and (4) to the solution of 3 was added 6.0 equiv. of [18]-crown-6. $[\mathbf{1}]_0$ = 3.0 mM.

4. UV-Vis spectrum of the complexes

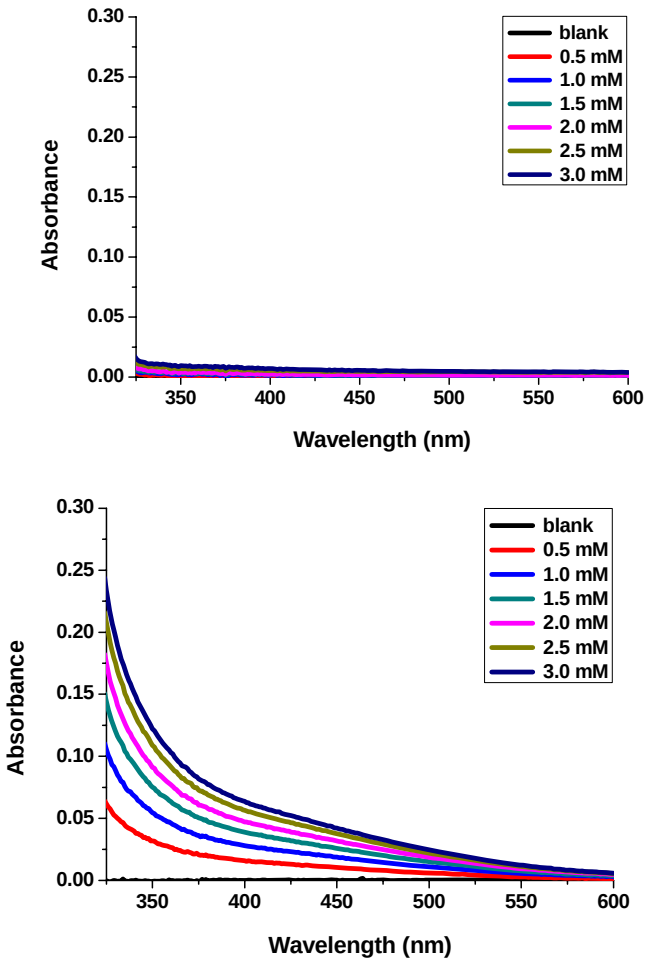

Fig. S34 UV/Vis absorption spectra of (top) free **2** by increasing its concentration, (bottom) **2** by increasing its concentration in the presence of **1** (1.0 mM, CH_3CN/CH_2Cl_2= 1:1, v/v).

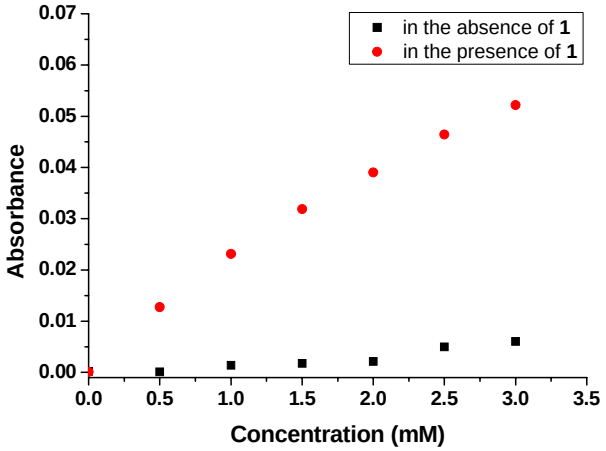

Fig. S35 Dependence of the absorbance at 425 nm of **2** on its concentration in the absence and presence of **1** (1.0 mM, CH_3CN/CH_2Cl_2= 1:1, v/v).

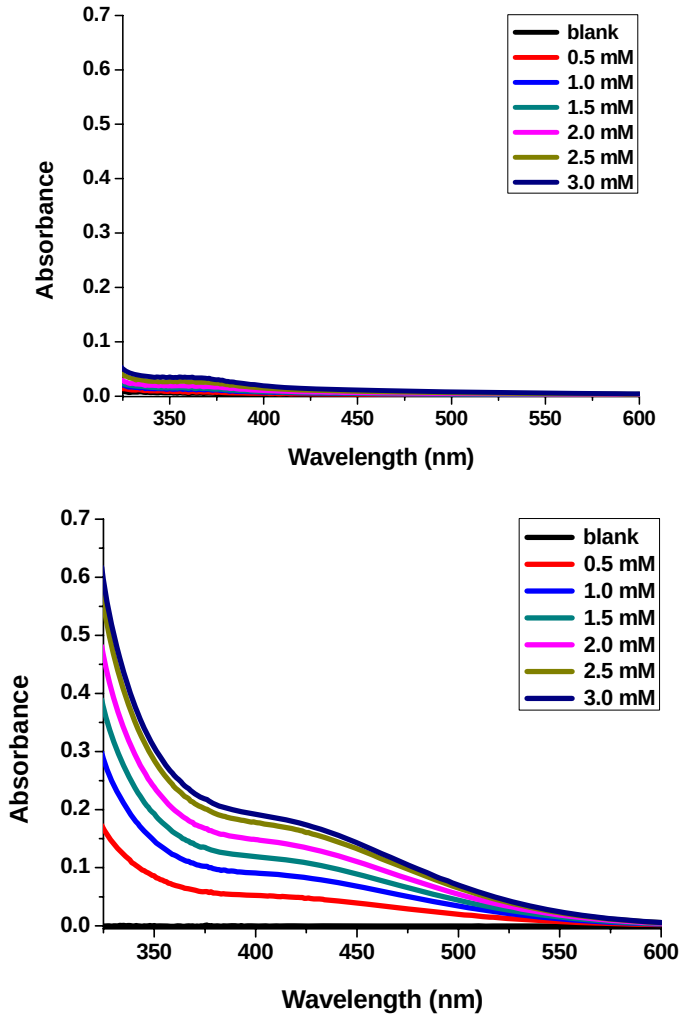

Fig. S36 UV/Vis absorption spectra of (top) free **3** by increasing its concentration, (bottom) **3** by increasing its concentration in the presence of **1** (1.0 mM, CH_3CN/CH_2Cl_2= 1:1, v/v).

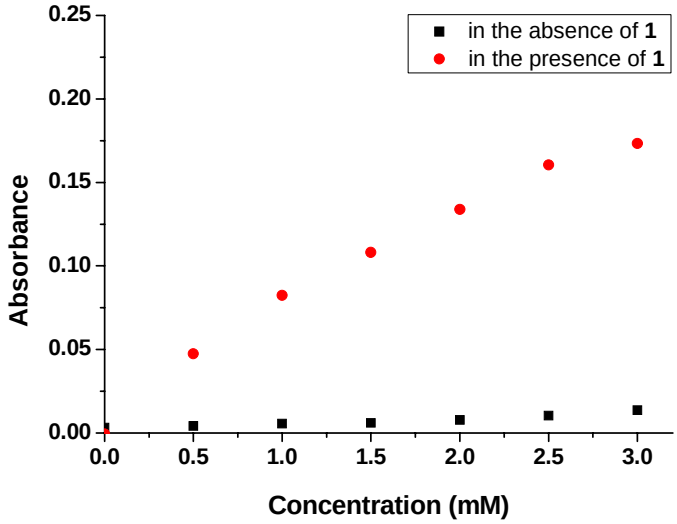

Fig. S37 Dependence of the absorbance at 425 nm of **3** on its concentration in the absence and presence of **1** (1.0 mM, CH_3CN/CH_2Cl_2= 1:1, v/v).

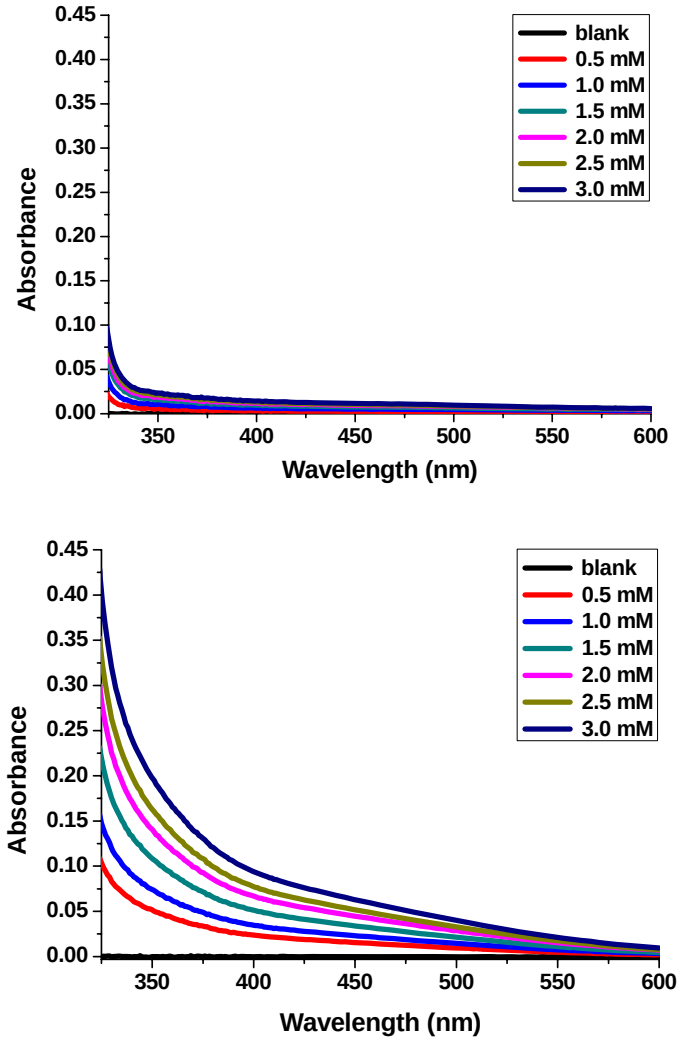

Fig. S38 UV/Vis absorption spectra of (top) free **4** by increasing its concentration, (bottom) **4** by increasing its concentration in the presence of **1** (1.0 mM, CH_3CN/CH_2Cl_2= 1:1, v/v).

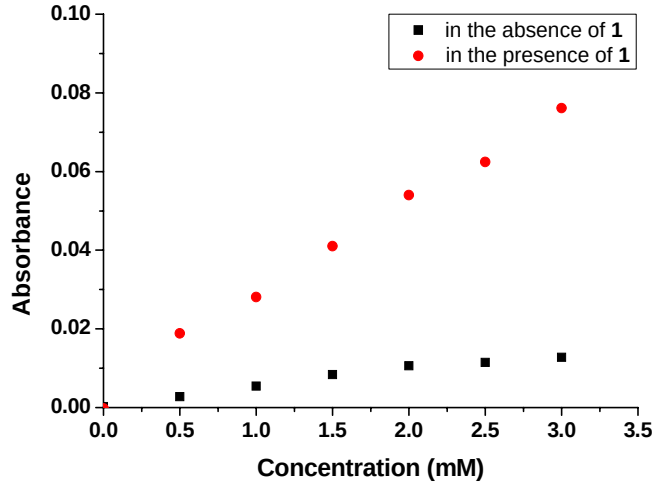

Fig. S39 Dependence of the absorbance at 425 nm of **4** on its concentration in the absence and presence of **1** (1.0 mM, CH_3CN/CH_2Cl_2= 1:1, v/v).

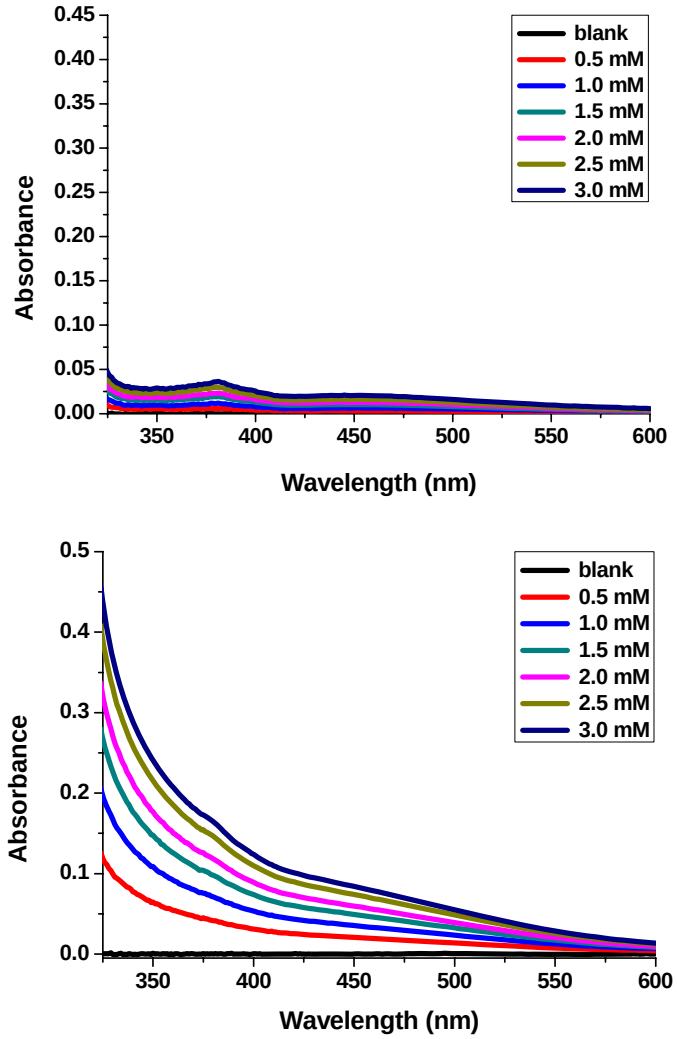

Fig. S40 UV/Vis absorption spectra of (top) free **5** by increasing its concentration, (bottom) **5** by increasing its concentration in the presence of **1** (1.0 mM, CH_3CN/CH_2Cl_2= 1:1, v/v).

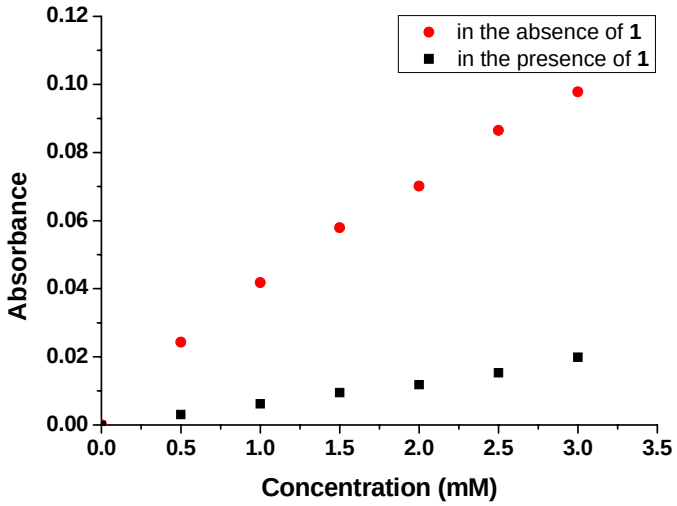

Fig. S41 Dependence of the absorbance at 425 nm of **5** on its concentration in the absence and presence of **1** (1.0 mM, CH_3CN/CH_2Cl_2= 1:1, v/v).

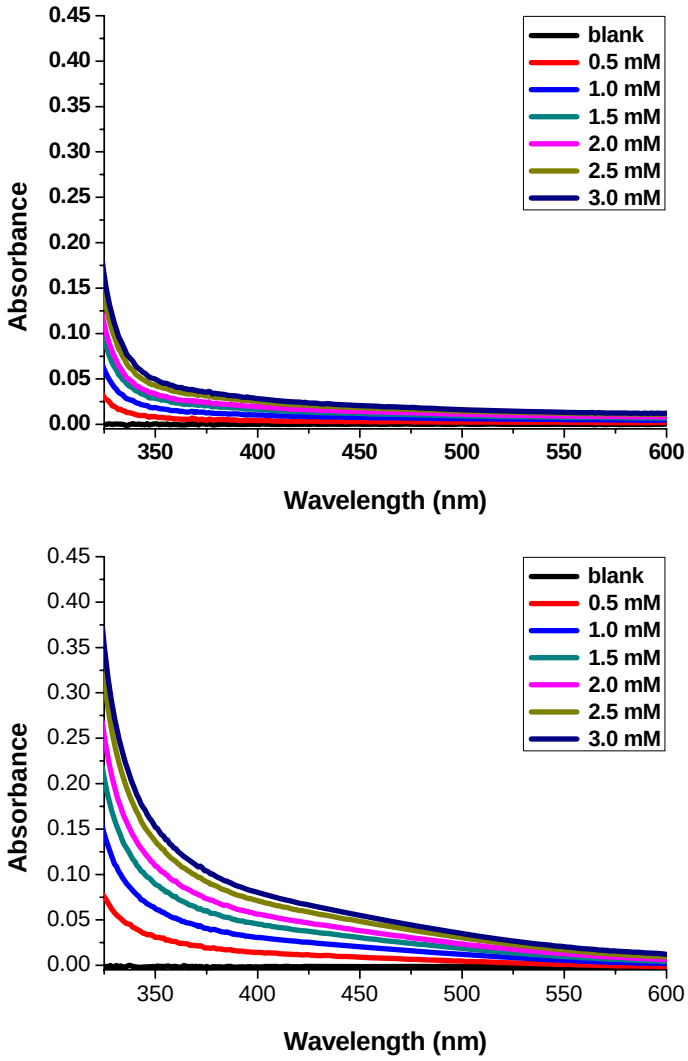

Fig. S42 UV/Vis absorption spectra of (top) free **6** by increasing its concentration, (bottom) **6** by increasing its concentration in the presence of **1** (1.0 mM, CH_3CN/CH_2Cl_2= 1:1, v/v).

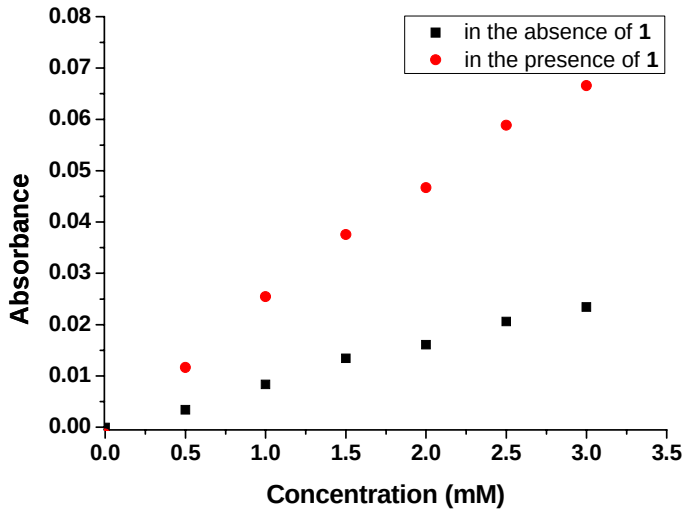

Fig. S43 Dependence of the absorbance at 425 nm of **6** on its concentration in the absence and presence of **1** (1.0 mM, CH_3CN/CH_2Cl_2= 1:1, v/v).

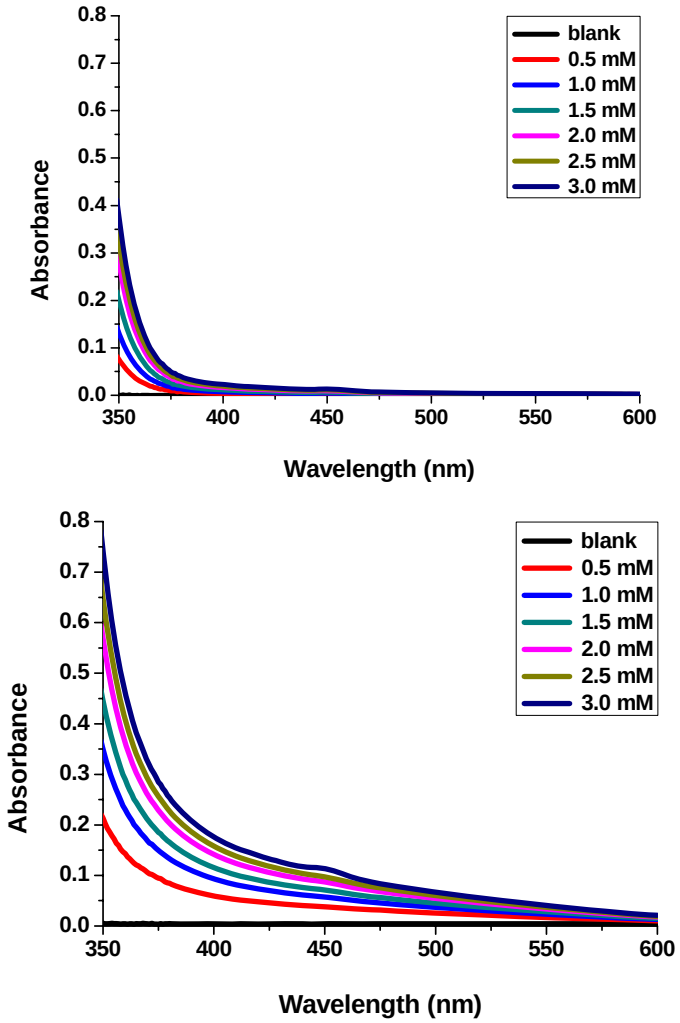

Fig. S44 UV/Vis absorption spectra of (top) free **7** by increasing its concentration, (bottom) **7** by increasing its concentration in the presence of **1** (1.0 mM, CH_3CN/CH_2Cl_2= 1:1, v/v).

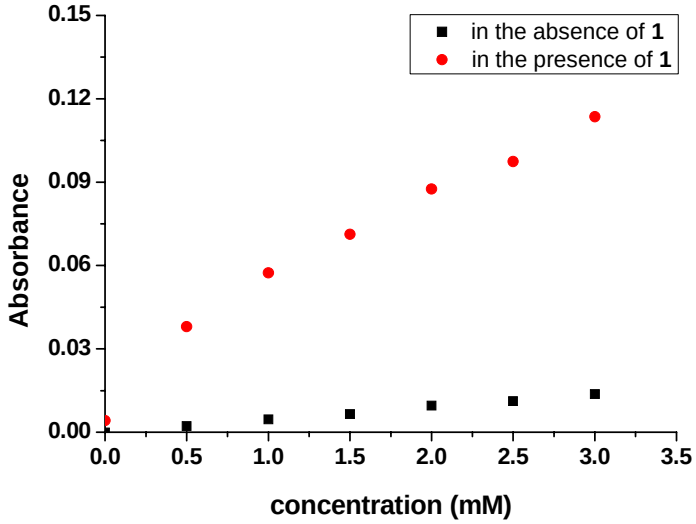

Fig. S45 Dependence of the absorbance at 425 nm of **7** on its concentration in the absence and presence of **1** (1.0 mM, CH_3CN/CH_2Cl_2= 1:1, v/v).

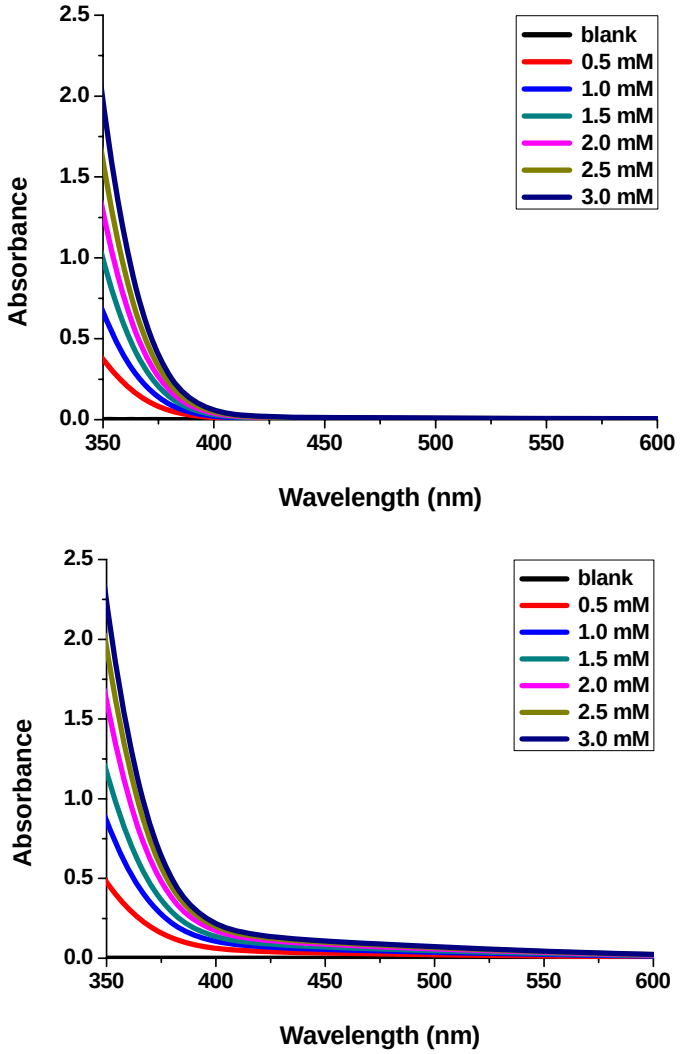

Fig. S46 UV/Vis absorption spectra of (top) free **8** by increasing its concentration, (bottom) **8** by increasing its concentration in the presence of **1** (1.0 mM, CH_3CN/CH_2Cl_2= 1:1, v/v).

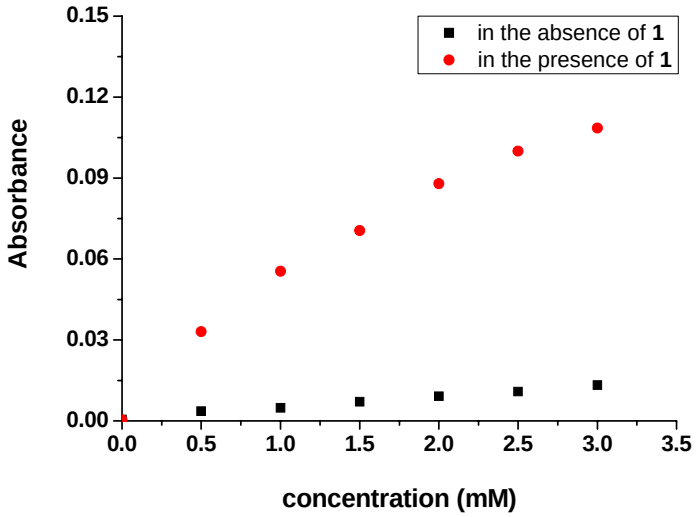

Fig. S47 Dependence of the absorbance at 425 nm of **8** on its concentration in the absence and presence of **1** (1.0 mM, CH_3CN/CH_2Cl_2= 1:1, v/v).

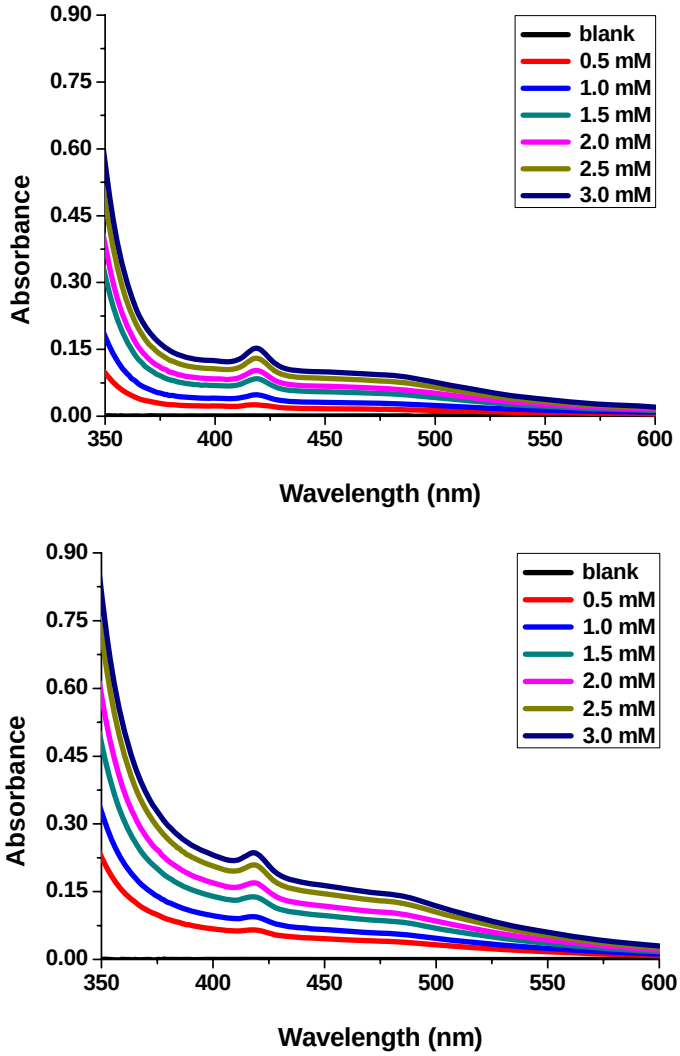

Fig. S48 UV/Vis absorption spectra of (top) free **9** by increasing its concentration, (bottom) **9** by increasing its concentration in the presence of **1** (1.0 mM, CH_3CN/CH_2Cl_2= 1:1, v/v).

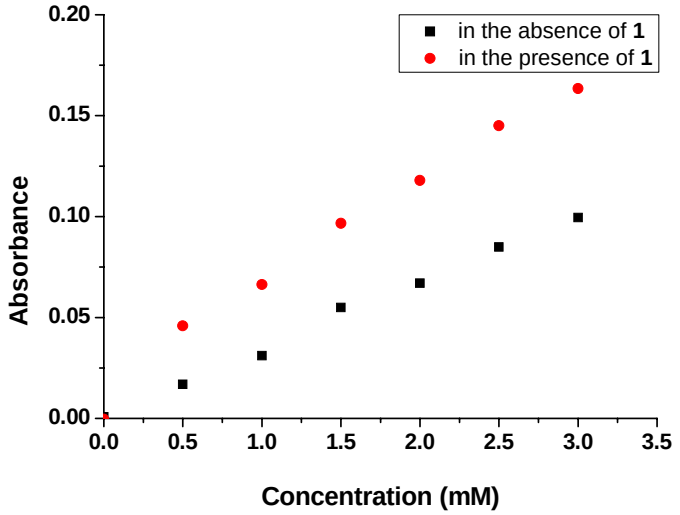

Fig. S49 Dependence of the absorbance at 450 nm of **9** on its concentration in the absence and presence of **1** (1.0 mM, CH_3CN/CH_2Cl_2= 1:1, v/v).

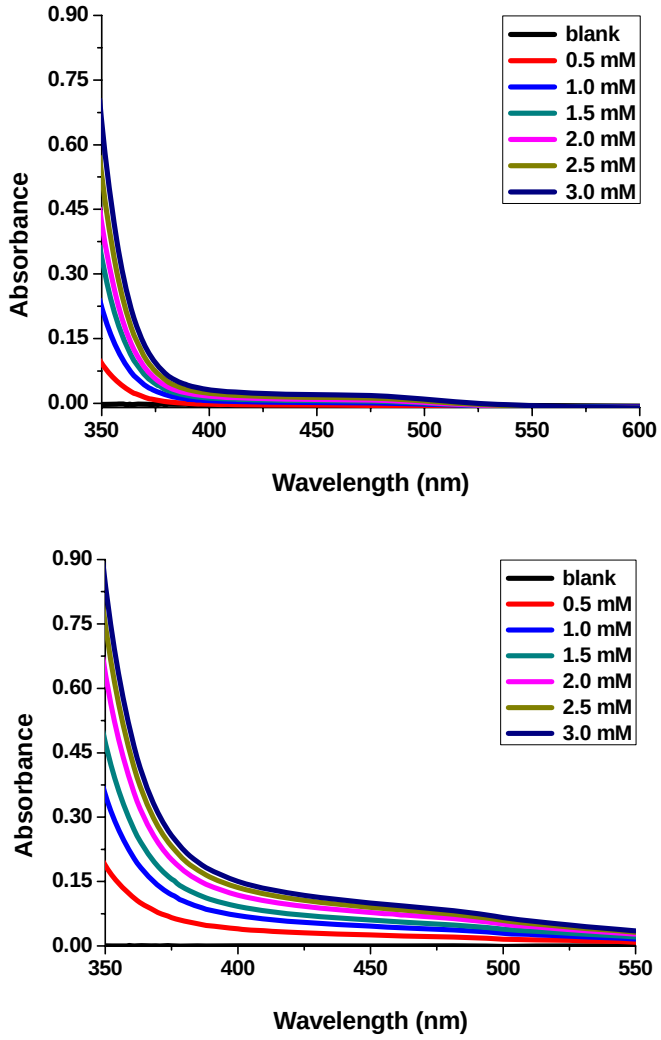

Fig. S50 UV/Vis absorption spectra of (top) free **10** by increasing its concentration, (bottom) **10** by increasing its concentration in the presence of **1** (1.0 mM, CH_3CN/CH_2Cl_2= 1:1, v/v).

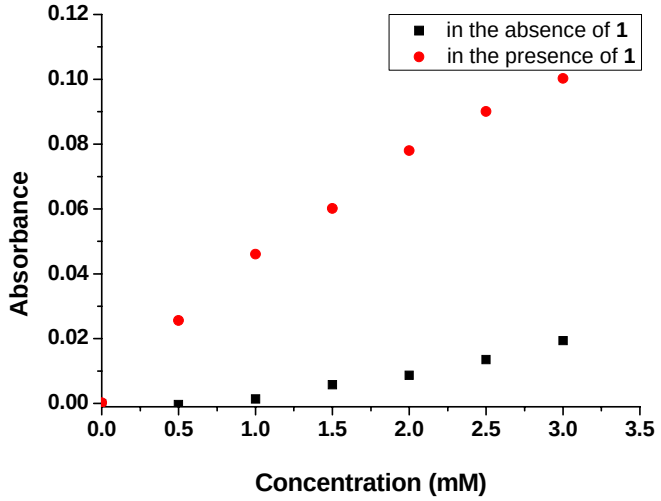

Fig. S51 Dependence of the absorbance at 450 nm of **10** on its concentration in the absence and presence of **1** (1.0 mM, CH_3CN/CH_2Cl_2= 1:1, v/v).

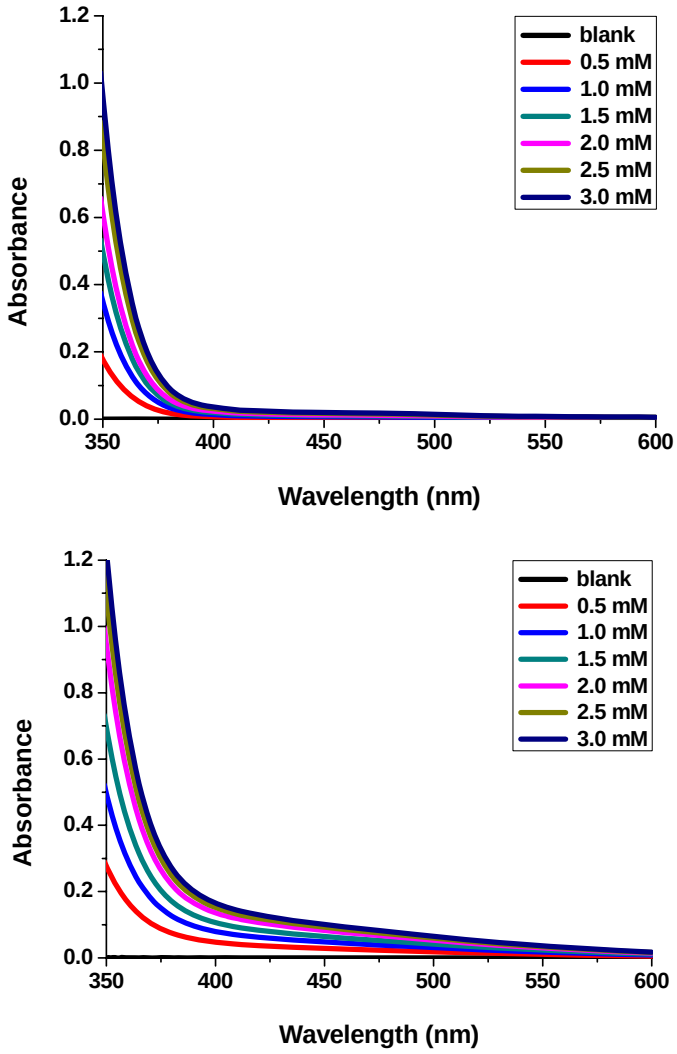

Fig. S52 UV/Vis absorption spectra of (top) free **11** by increasing its concentration, (bottom) **11** by increasing its concentration in the presence of **1** (1.0 mM, CH_3CN/CH_2Cl_2= 1:1, v/v).

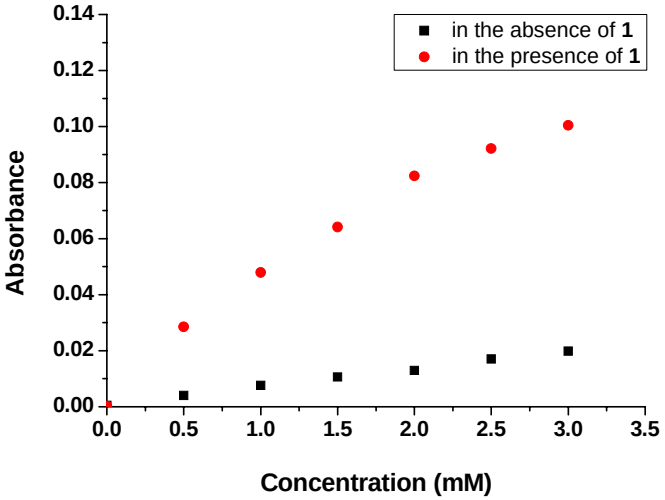

Fig. S53 Dependence of the absorbance at 450 nm of **11** on its concentration in the absence and presence of **1** (1.0 mM, CH_3CN/CH_2Cl_2= 1:1, v/v).

5. ESI-MS spectra of the complexes

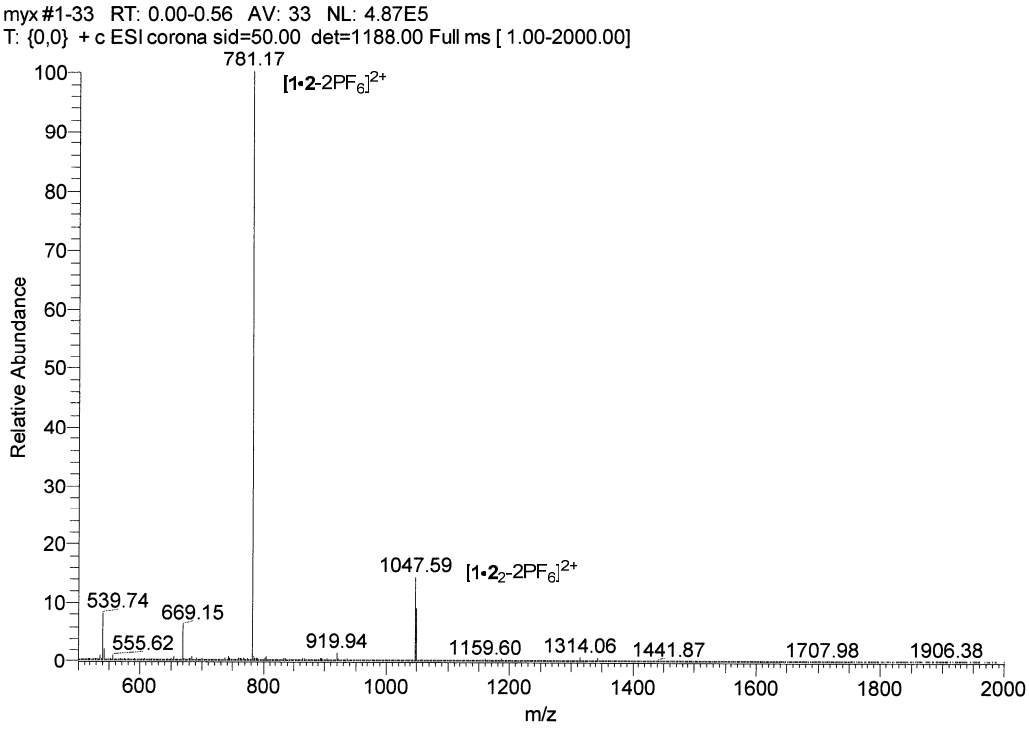

Fig. S54 ESI-MS of **1** and **2** in acetonitrile-chloroform (1:1, v:v).

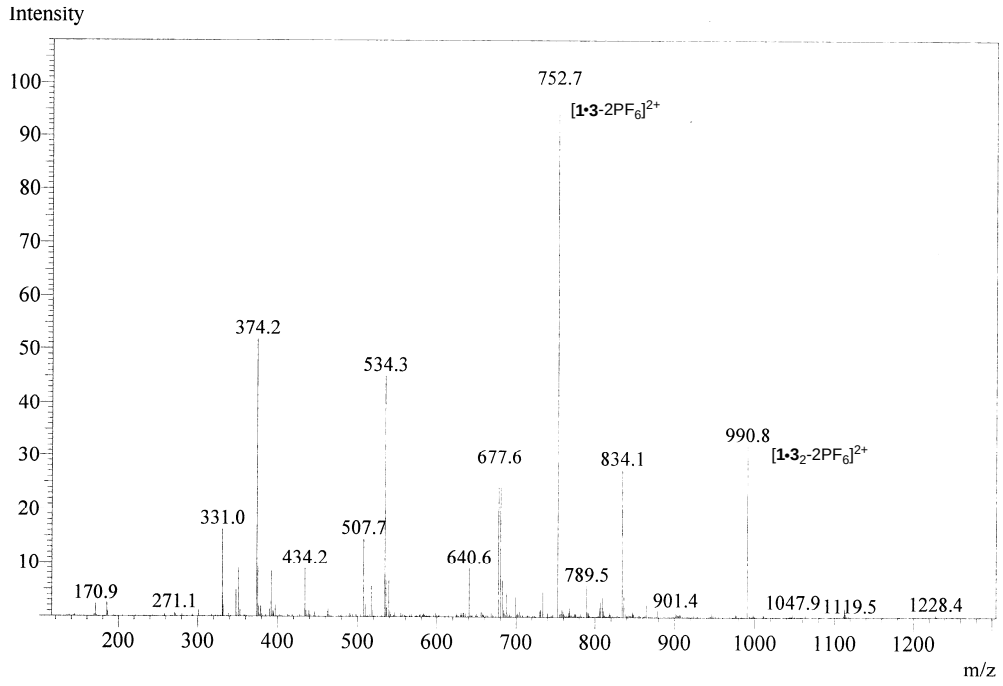

Fig. S55 ESI-MS of **1** and **3** in acetonitrile-chloroform (1:1, v:v).

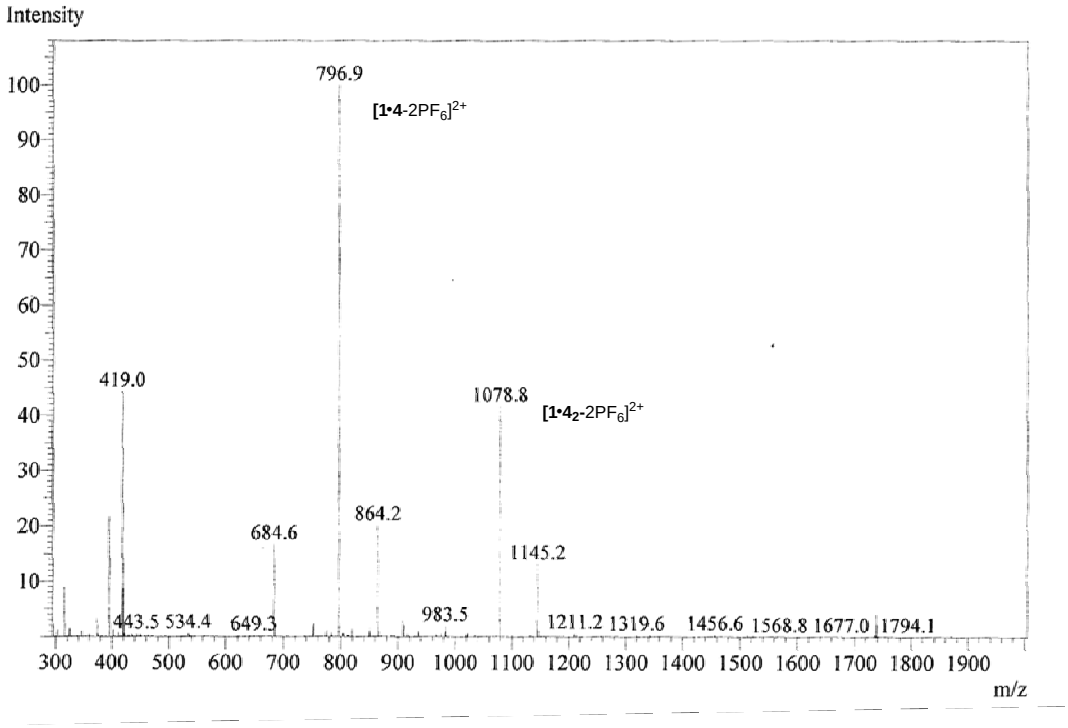

Fig. S56 ESI-MS of **1** and **4** in acetonitrile-chloroform (1:1, v:v).

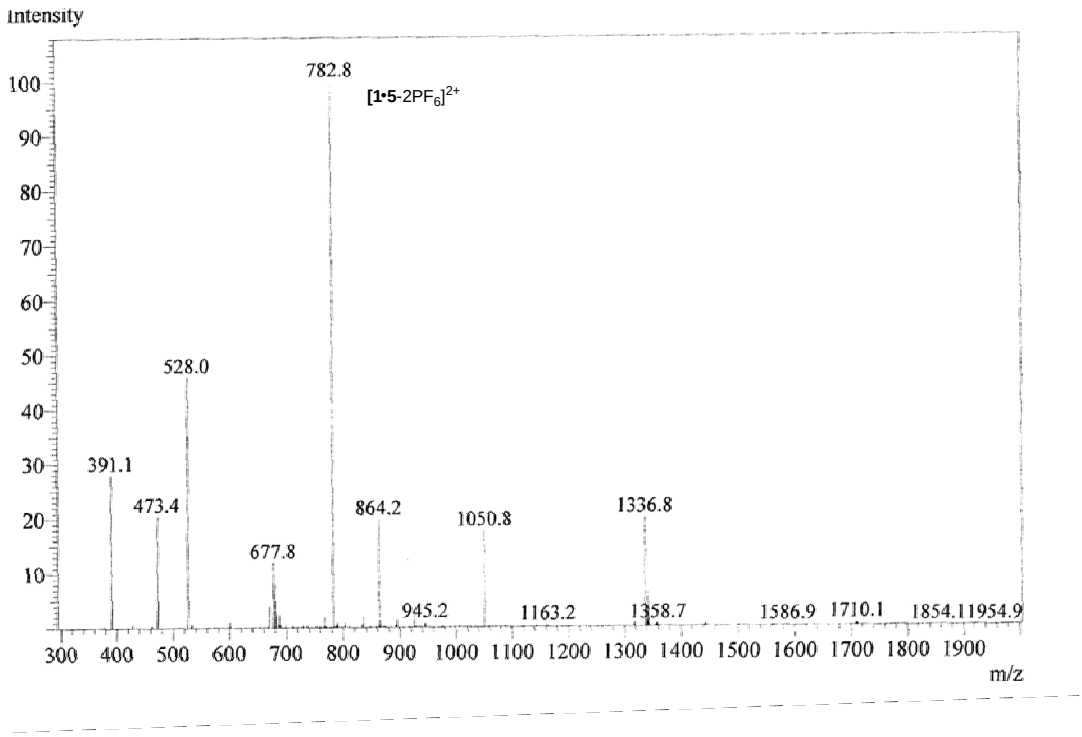

Fig. S57 ESI-MS of **1** and **5** in acetonitrile-chloroform (1:1, v:v).

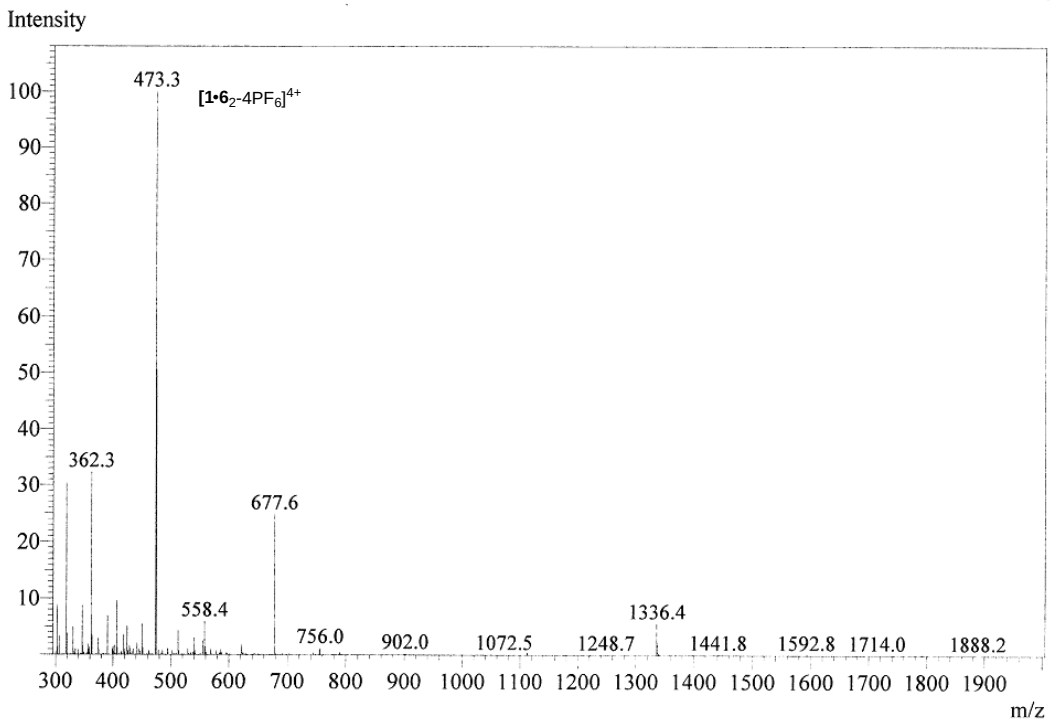

Fig. S58 ESI-MS of **1** and **6** in acetonitrile-chloroform (1:1, v:v).

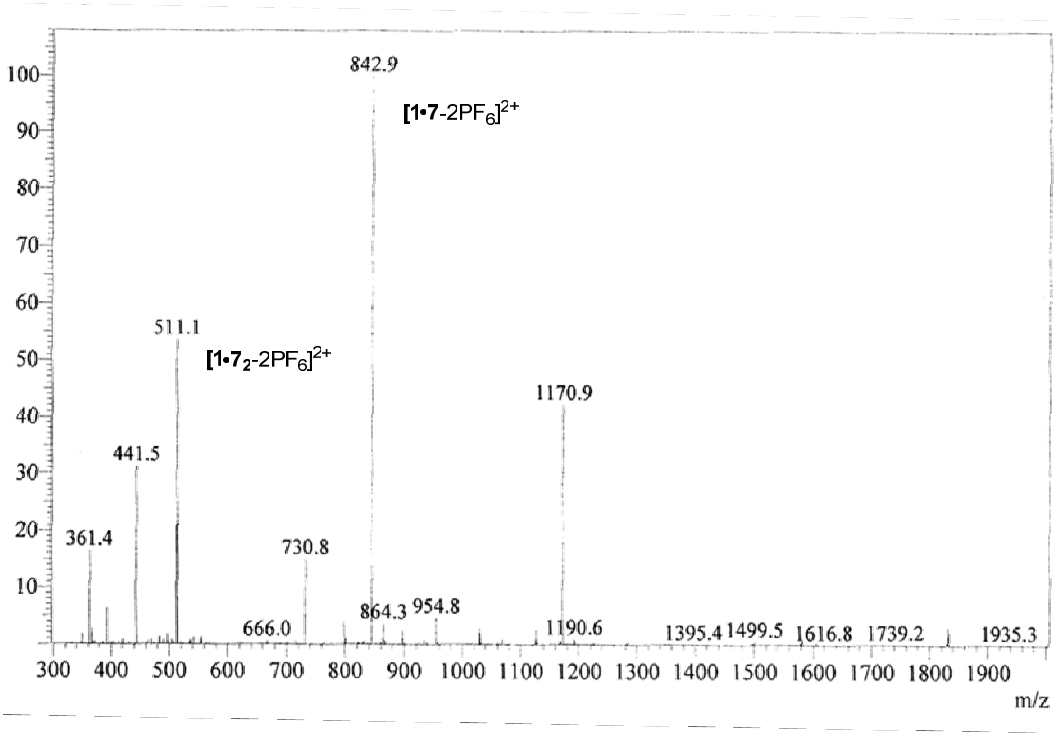

Fig. S59 ESI-MS of **1** and **7** in acetonitrile-chloroform (1:1, v:v).

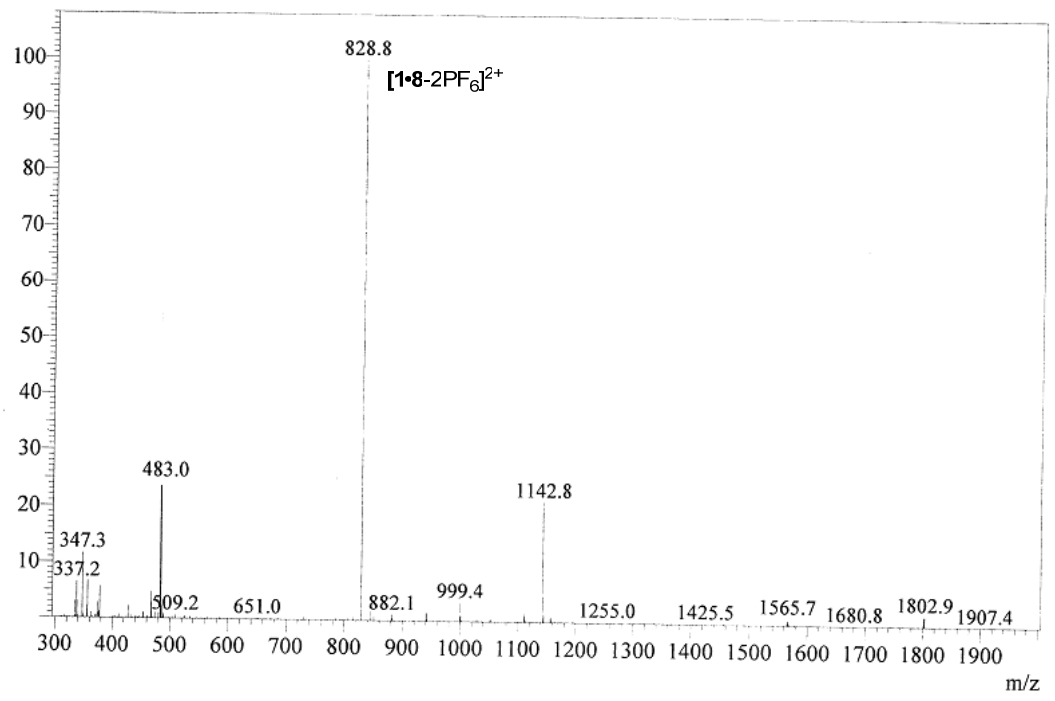

Fig. S60 ESI-MS of **1** and **8** in acetonitrile-chloroform (1:1, v:v).

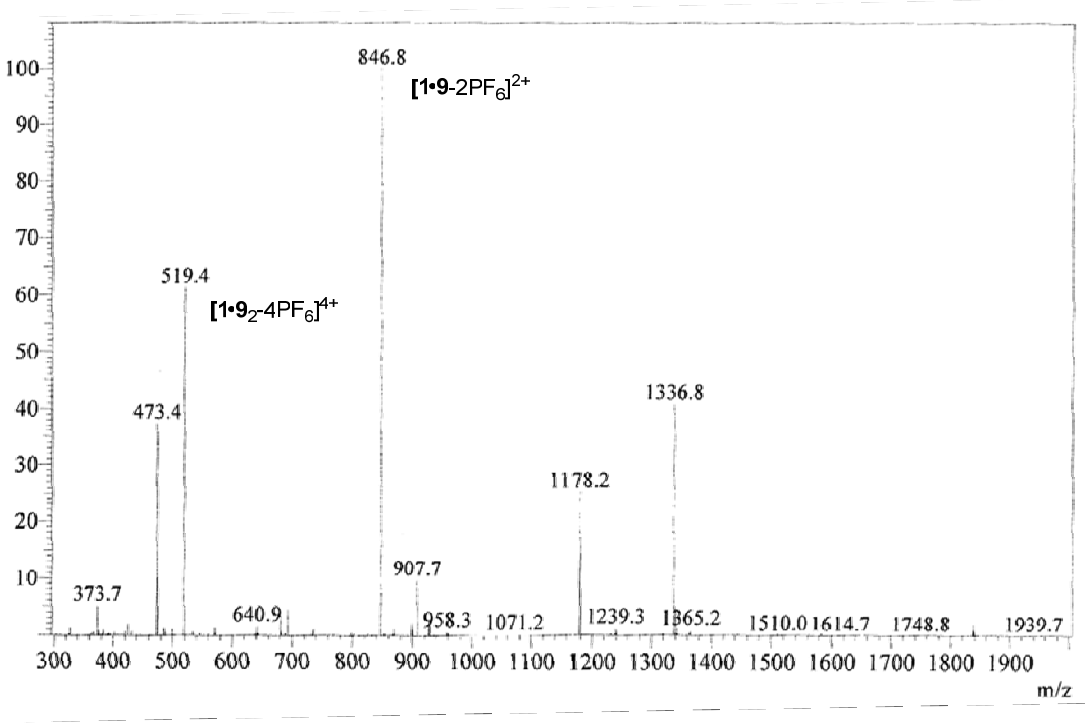

Fig. S61 ESI-MS of **1** and **9** in acetonitrile-chloroform (1:1, v:v).

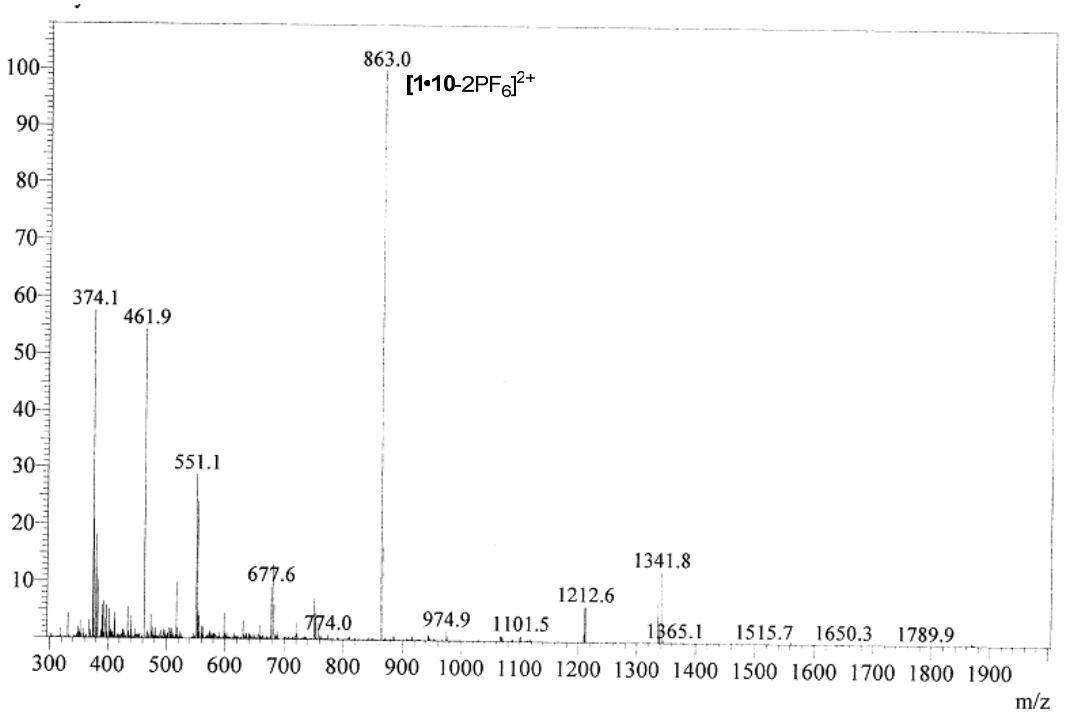

Fig. S62 ESI-MS of **1** and **10** in acetonitrile-chloroform (1:1, v:v).

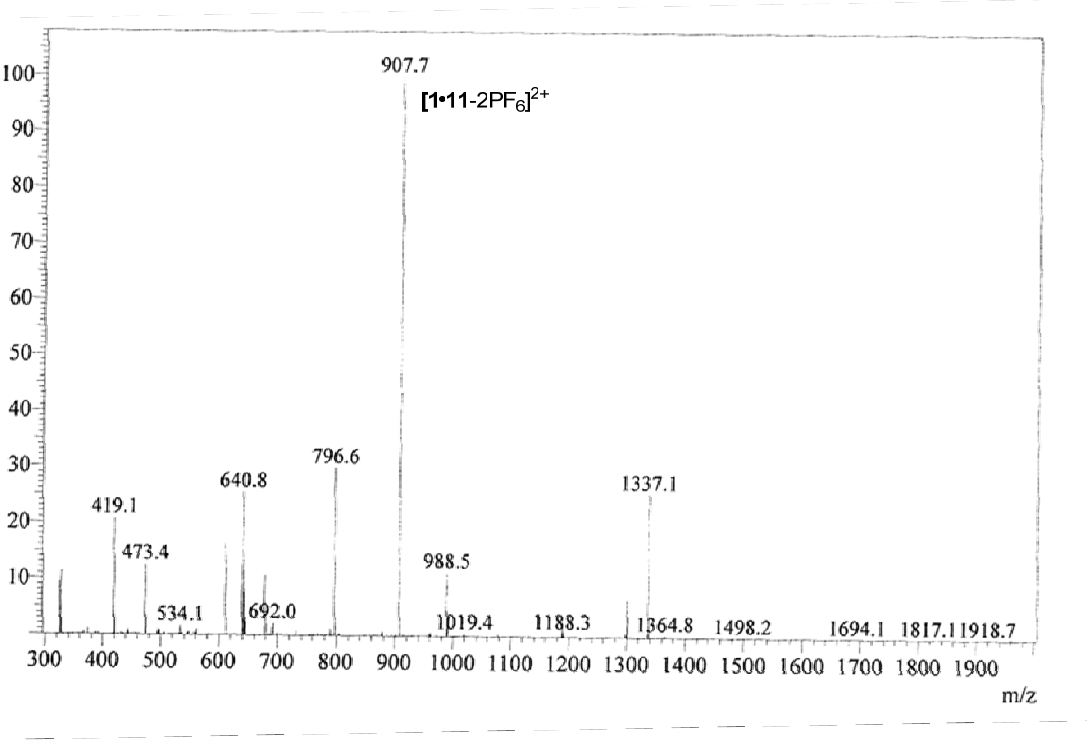

Fig. S63 ESI-MS of **1** and **11** in acetonitrile-chloroform (1:1, v:v).

6. ^{1}H-^{1}H COSY and ROESY spectra of the complexes

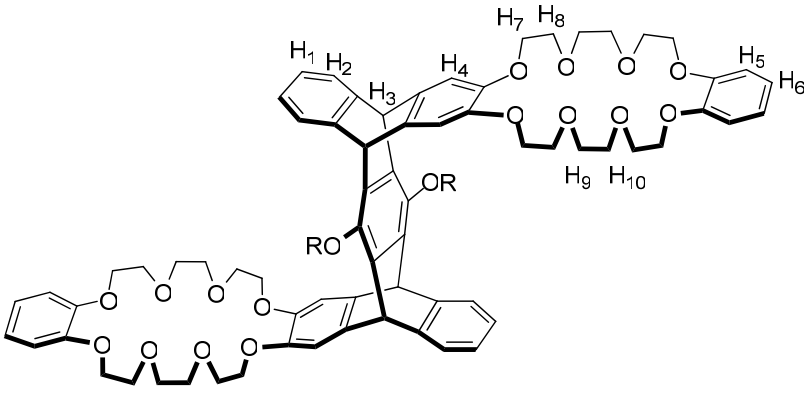

1 R = CH_2CH_2OMe

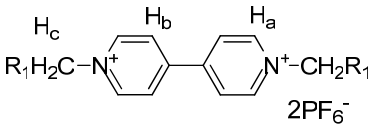

2 R_1 = CH_2CH_3
3 R_1 = H
4 R_1 = CH_2OCH_3
5 R_1 = CH_2OH
6 R_1 = $CH_2CH{=}CH_2$

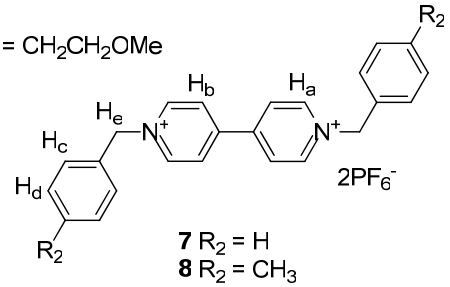

7 R_2 = H
8 R_2 = CH_3
9 R_2 = F
10 R_2 = Cl
11 R_2 = Br

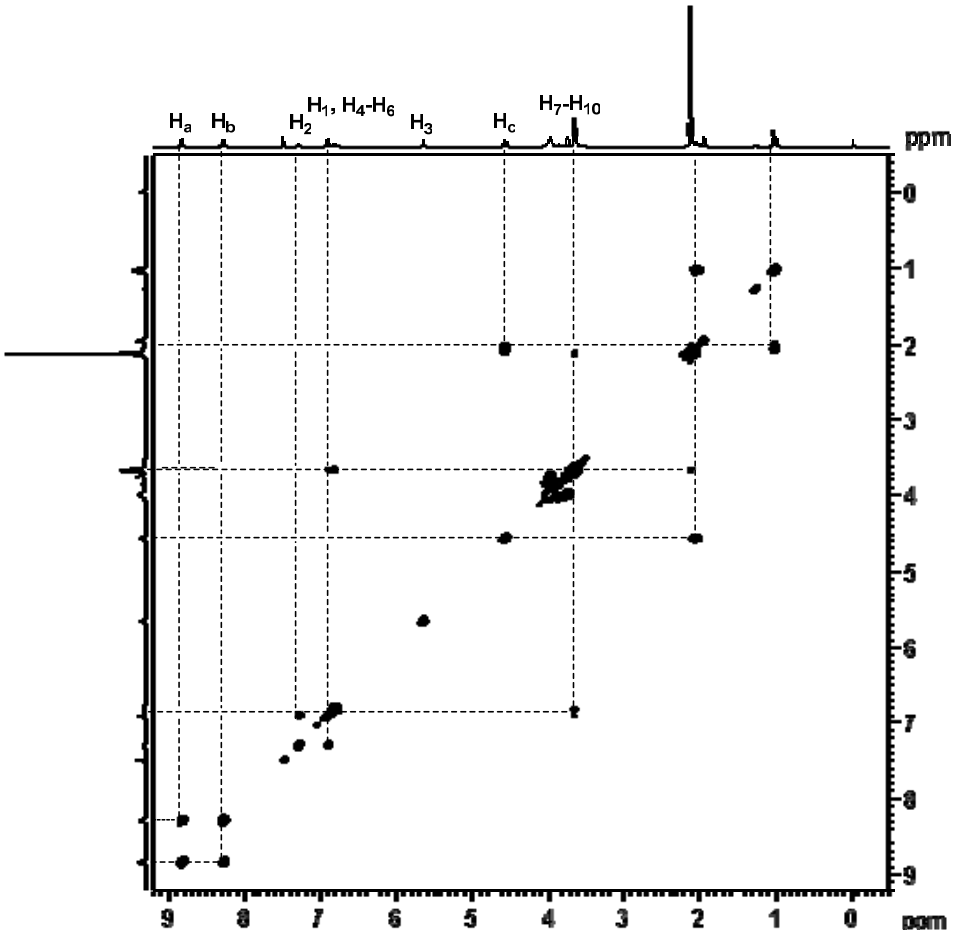

Fig. S64 ^{1}H-^{1}H COSY spectrum (600 MHz, $CD_3CN/CDCl_3$=1:1, v/v, 295K) of **1** and 2 equiv of **2**. $[\mathbf{1}]_0$ = 3.0 mM.

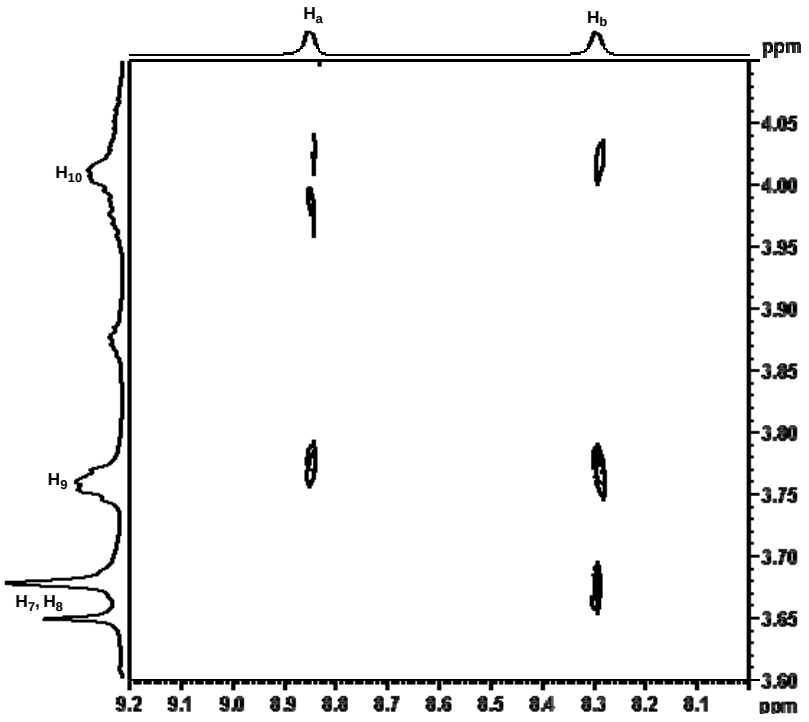

Fig. S65 ^{1}H-^{1}H ROESY spectrum (600 MHz, $CD_3CN/CDCl_3$=1:1, v/v, 295K) of **1** and 2 equiv of **2**. $[\mathbf{1}]_0$ = 3.0 mM.

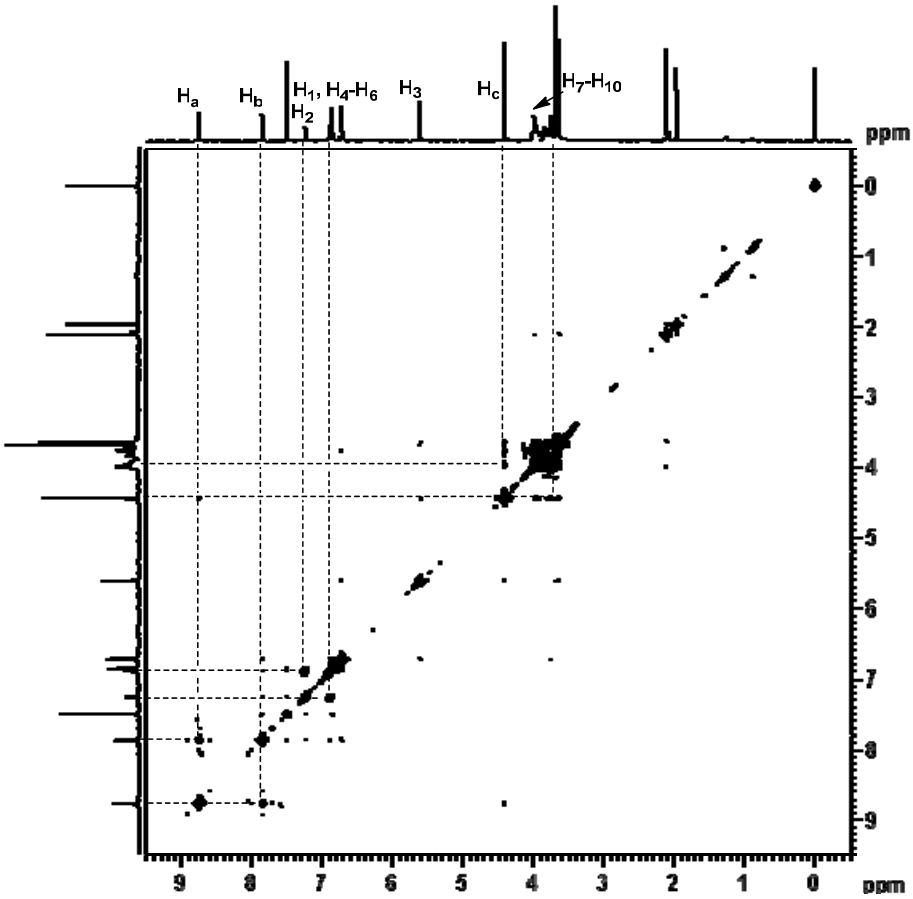

Fig. S66 ^{1}H-^{1}H COSY spectrum (600 MHz, $CD_3CN/CDCl_3$=1:1, v/v, 295K) of **1** and 2 equiv of **3**. $[\mathbf{1}]_0$ = 3.0 mM.

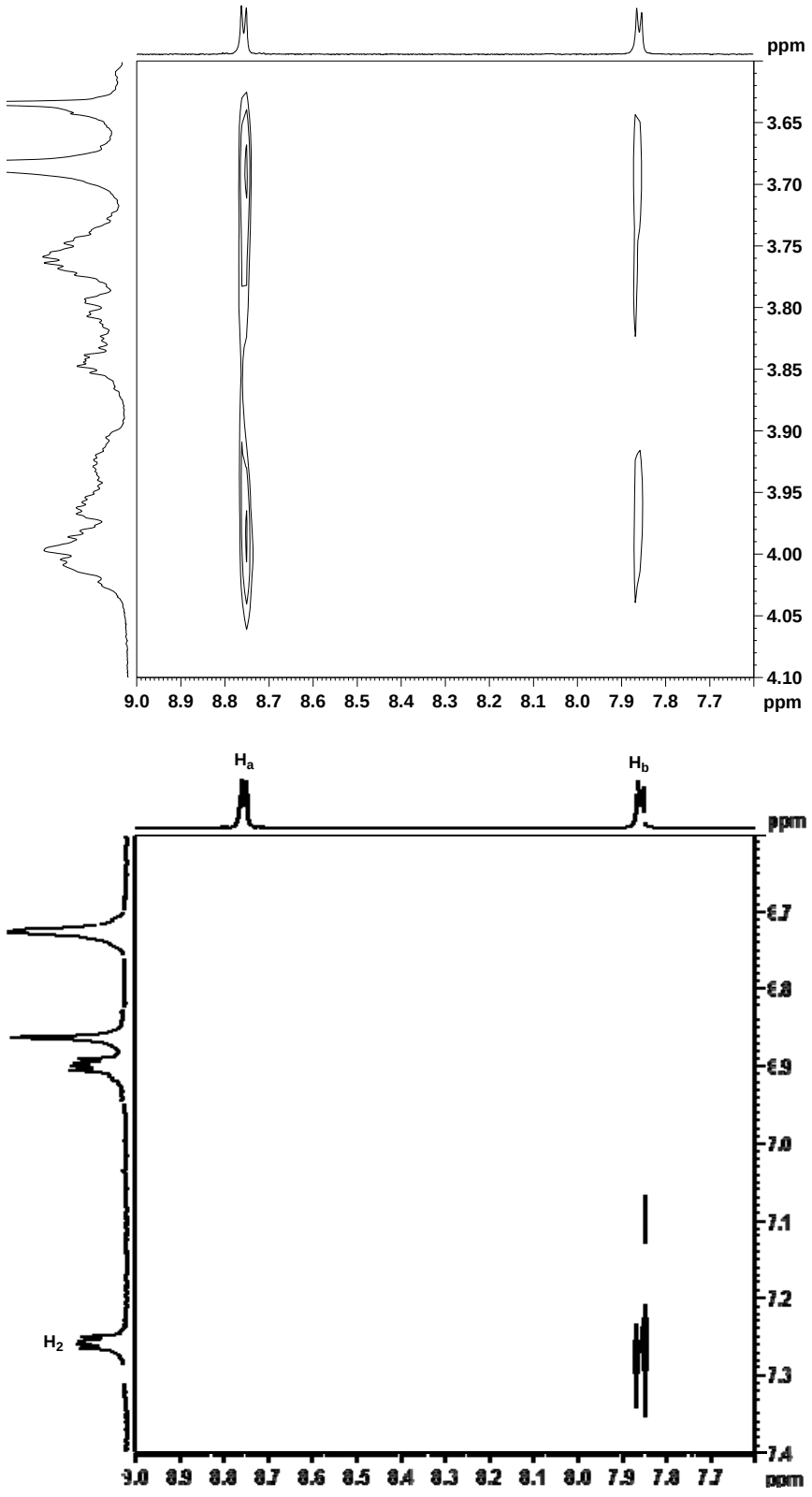

Fig. S67 ^{1}H-^{1}H ROESY spectrum (600 MHz, $CD_3CN/CDCl_3$=1:1, v/v, 295K) of **1** and 2 equiv of **3**. $[\mathbf{1}]_0$ = 3.0 mM.

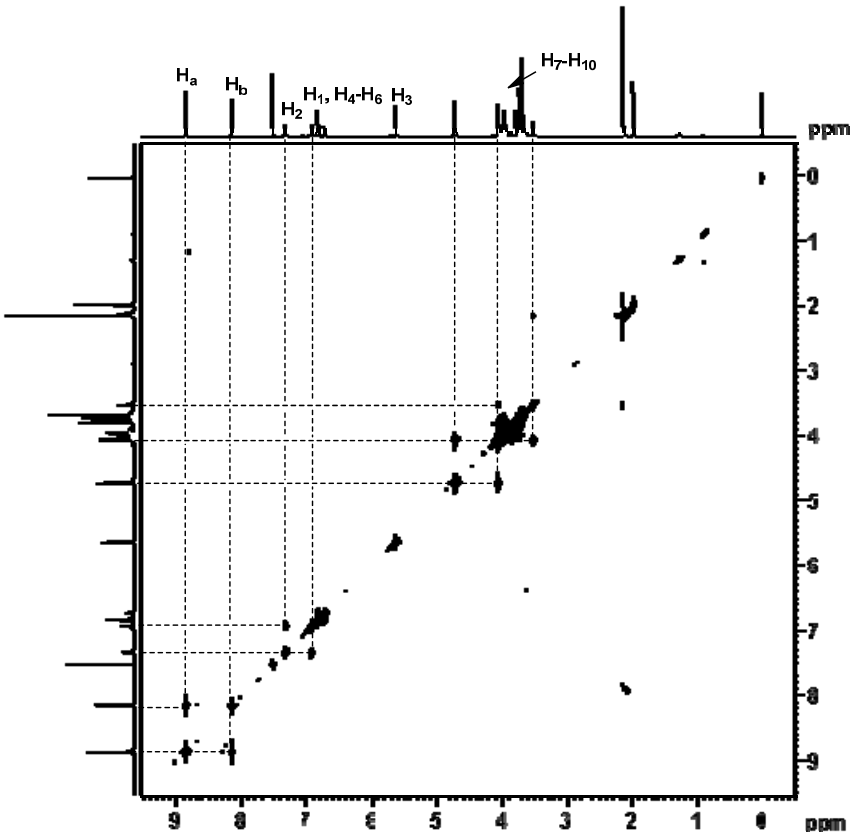

Fig. S68 ^{1}H-^{1}H COSY spectrum (600 MHz, $CD_3CN/CDCl_3$=1:1, v/v, 295K) of **1** and 2 equiv of **5**. $[\mathbf{1}]_0$ = 3.0 mM.

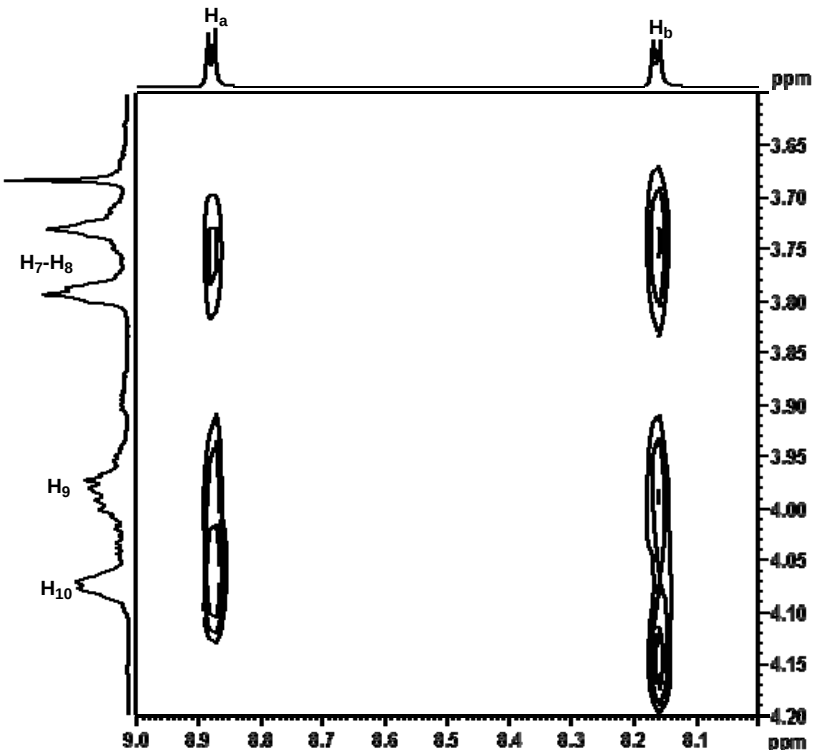

Fig. S69 ^{1}H-^{1}H ROESY spectrum (600 MHz, $CD_3CN/CDCl_3$=1:1, v/v, 295K) of **1** and 2 equiv of **5**. $[\mathbf{1}]_0$ = 3.0 mM.

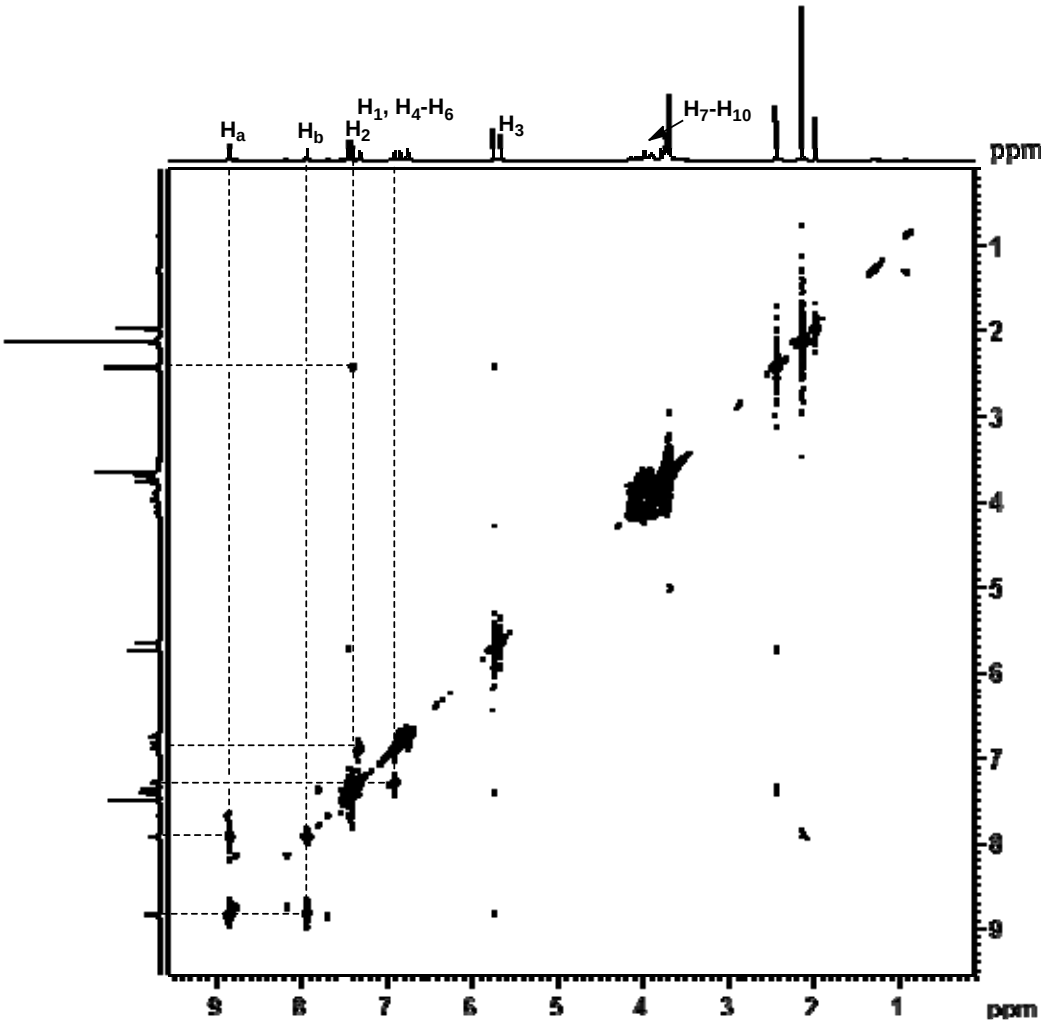

Fig. S70 ^{1}H-^{1}H COSY spectrum (600 MHz, $CD_3CN/CDCl_3$=1:1, v/v, 295K) of **1** and 2 equiv of **8**. $[\mathbf{1}]_0$ = 3.0 mM.

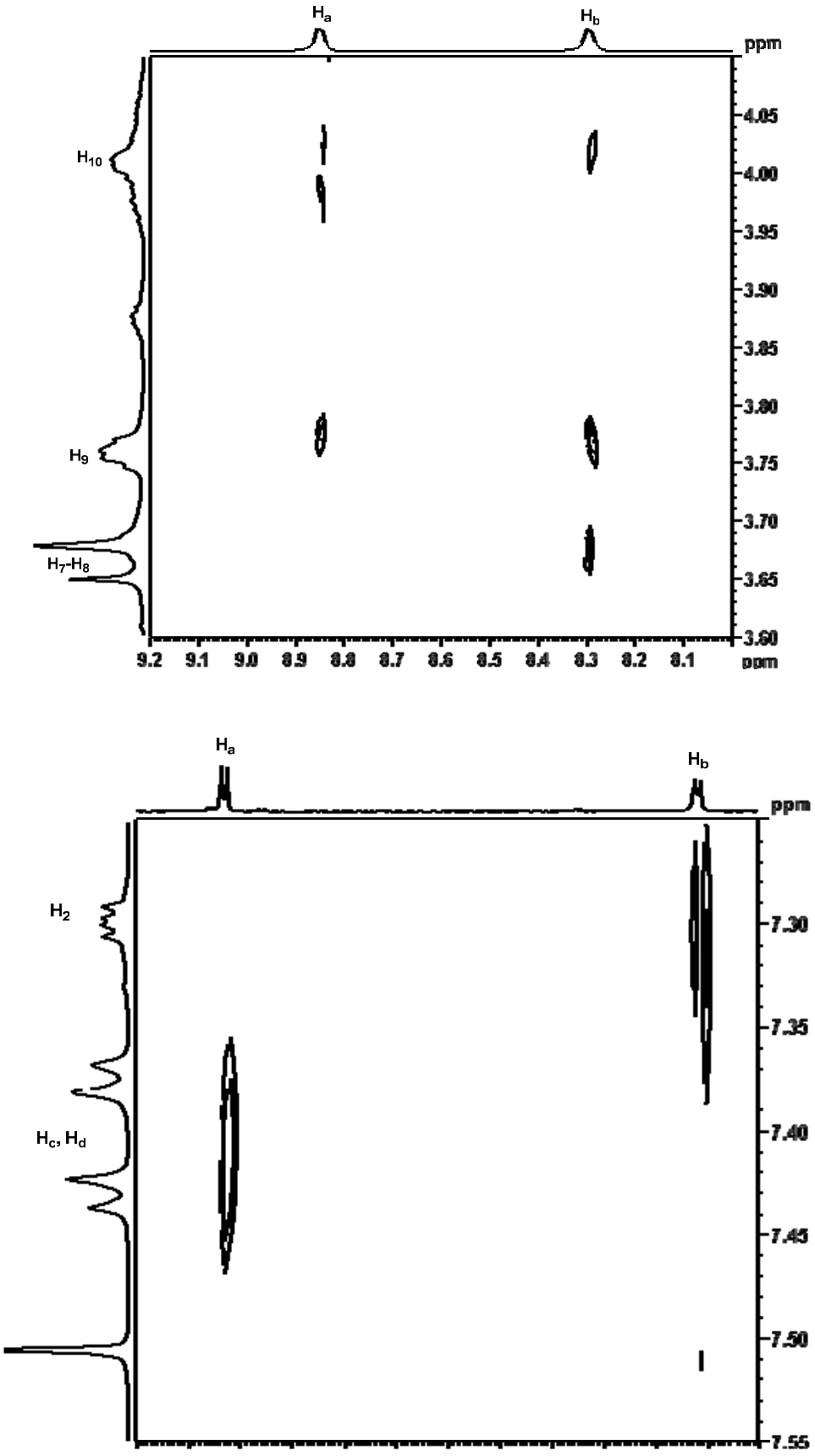

Fig. S71 ^{1}H-^{1}H ROESY spectrum (600 MHz, $CD_3CN/CDCl_3$=1:1, v/v, 295K) of **1** and 2 equiv of **8**. $[\mathbf{1}]_0$ = 3.0 mM.

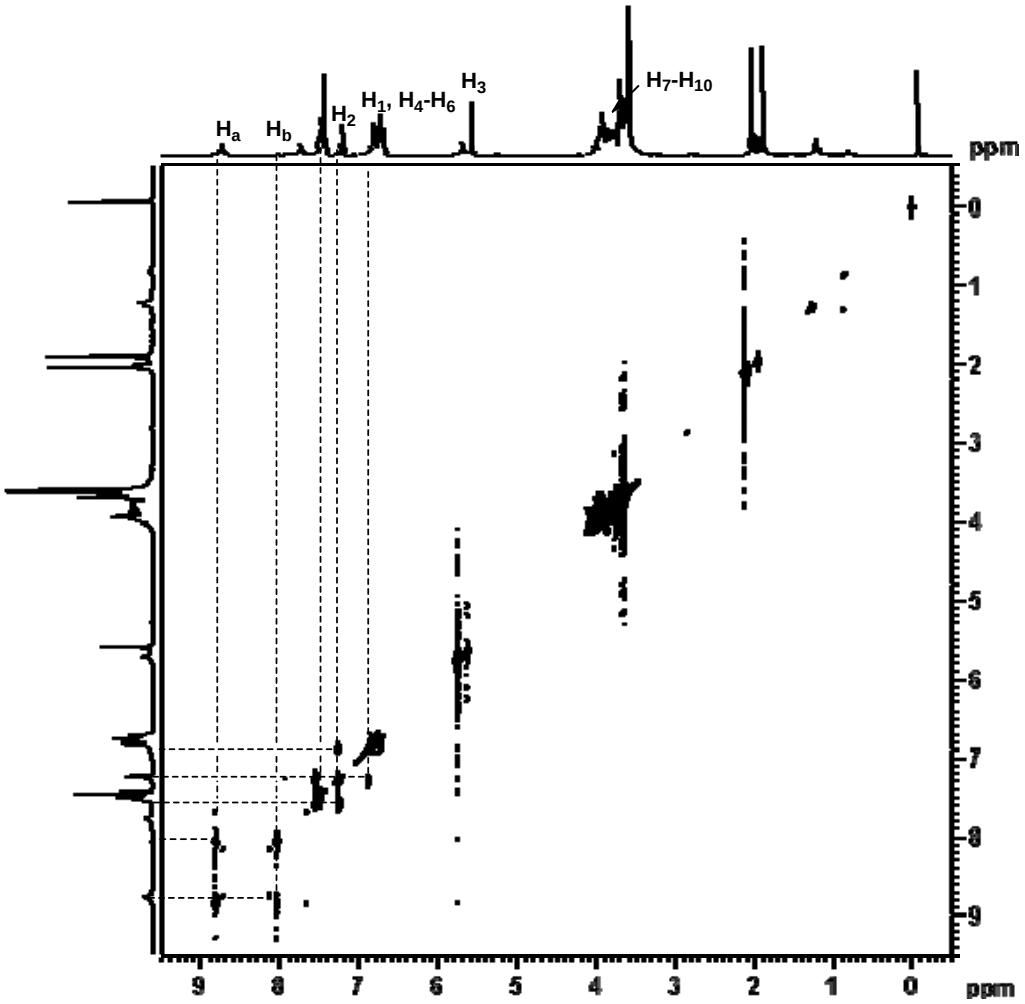

Fig. S72 ^{1}H-^{1}H COSY spectrum (600 MHz, $CD_3CN/CDCl_3$=1:1, v/v, 295K) of **1** and 2 equiv of **9**. $[\mathbf{1}]_0$ = 3.0 mM.

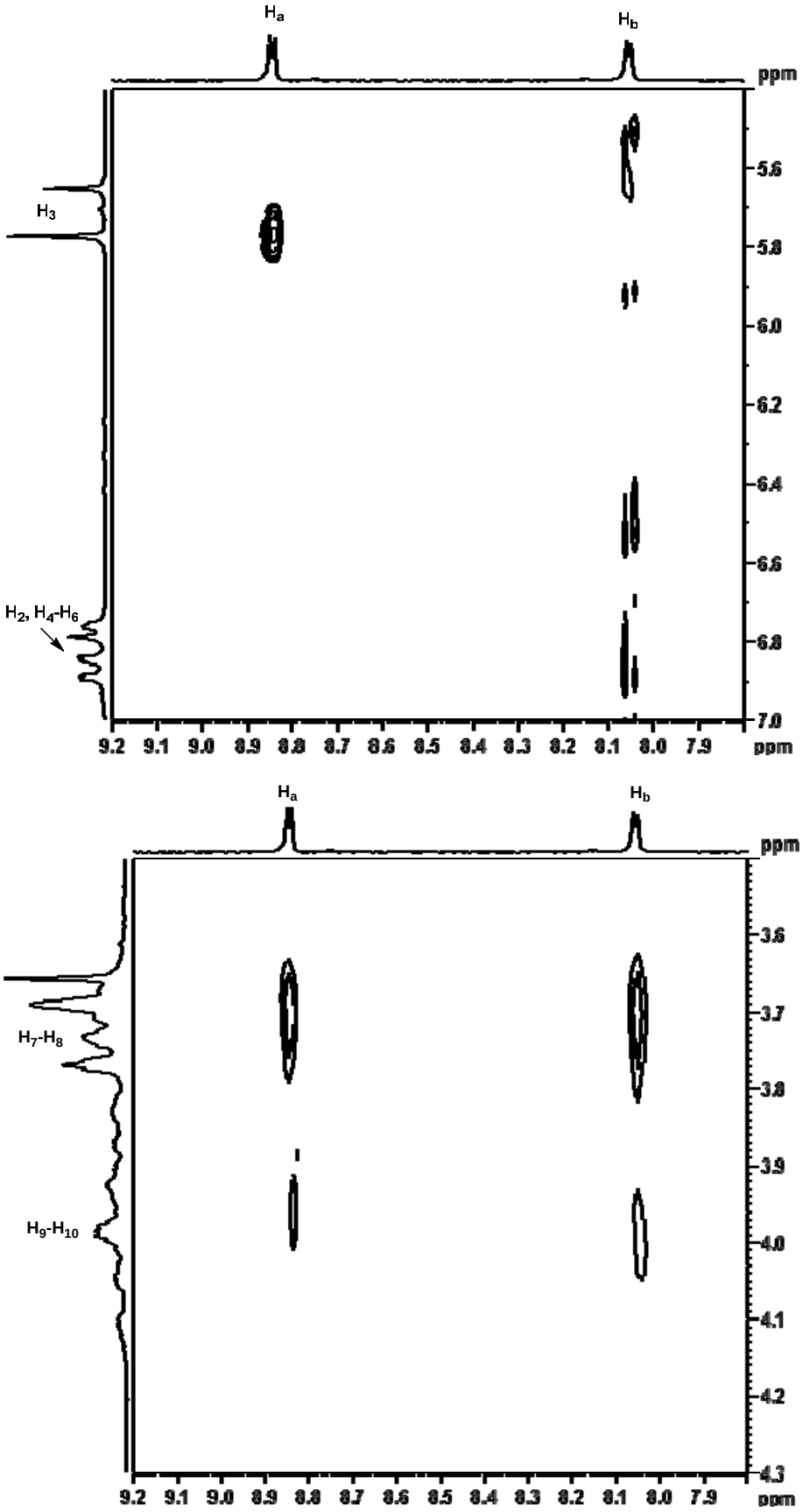

Fig. S73 ^{1}H-^{1}H ROESY spectrum (600 MHz, $CD_3CN/CDCl_3$=1:1, v/v, 295K) of **1** and 2 equiv of **9**. $[\mathbf{1}]_0$ = 3.0 mM.

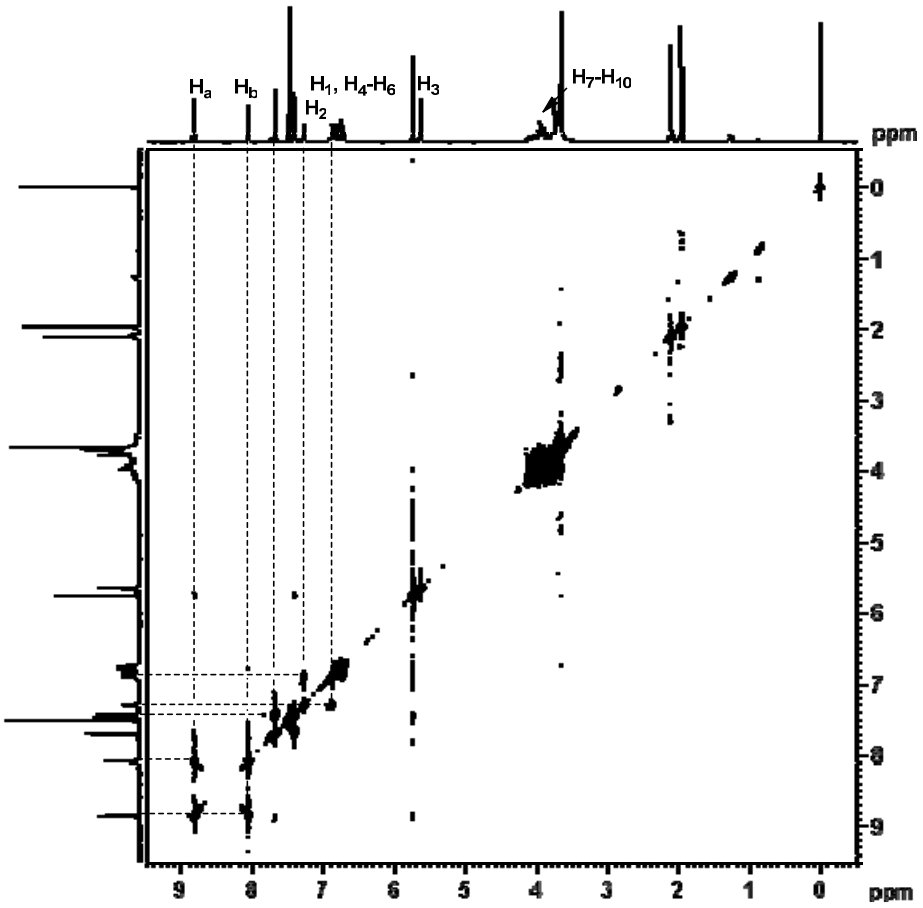

Fig. S74 ^{1}H-^{1}H COSY spectrum (600 MHz, $CD_3CN/CDCl_3$=1:1, v/v, 295K) of **1** and 2 equiv of **11**. $[\mathbf{1}]_0$ = 3.0 mM.

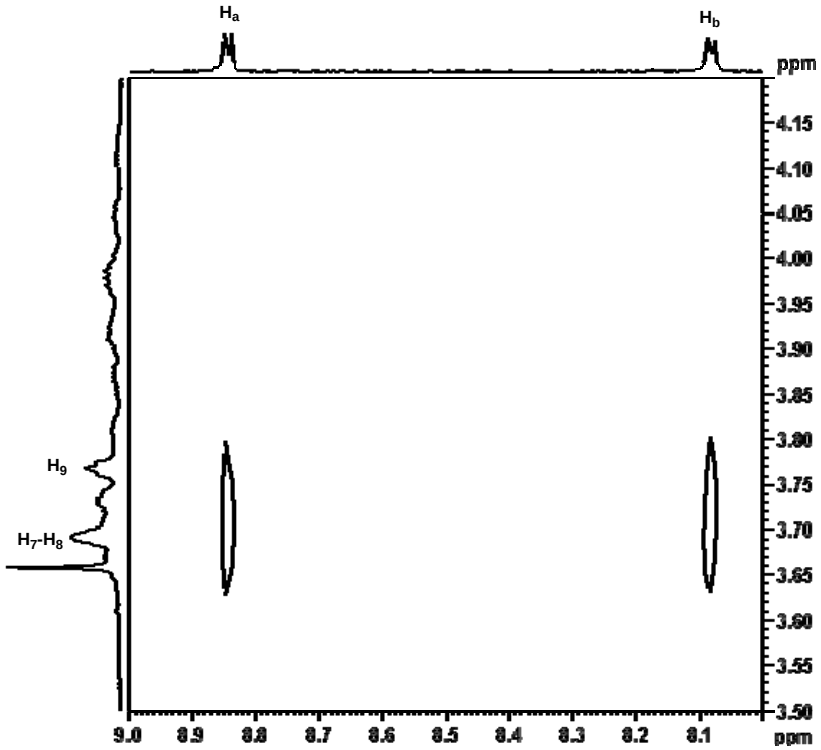

Fig. S75 ^{1}H-^{1}H ROESY spectrum (600 MHz, $CD_3CN/CDCl_3$=1:1, v/v, 295K) of **1** and 2 equiv of **11**. $[\mathbf{1}]_0$ = 3.0 mM.

7. Crystal structures and packing of the complexes

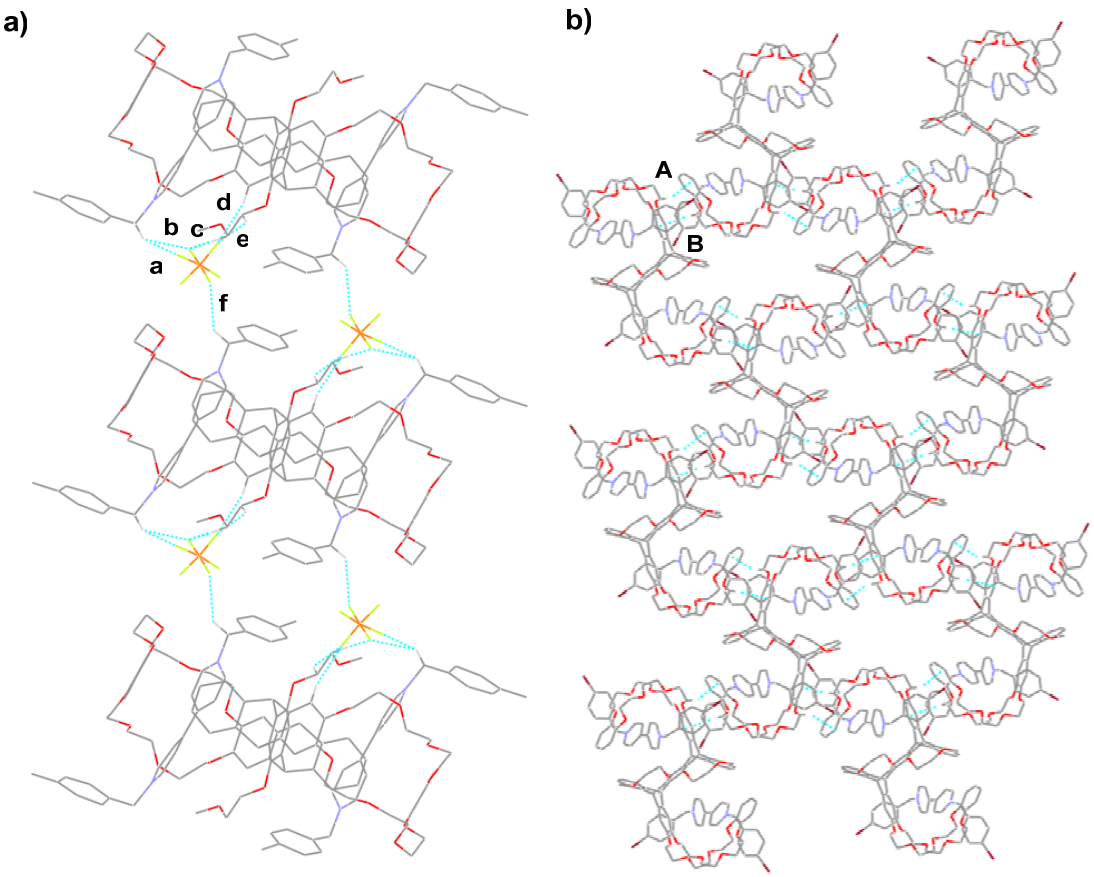

Fig. S76 (a) Linear supramolecular array of complex **1•8**$_2$ viewed along the *a* axis and (b) packing of the complex **1•11**$_2$ viewed along the a axis. Blue lines denote the non-covalent interactions between the host and the guests. Solvent molecules, PF_6 counterions, and hydrogen atoms not involved in the non-covalent interactions were omitted for clarity.

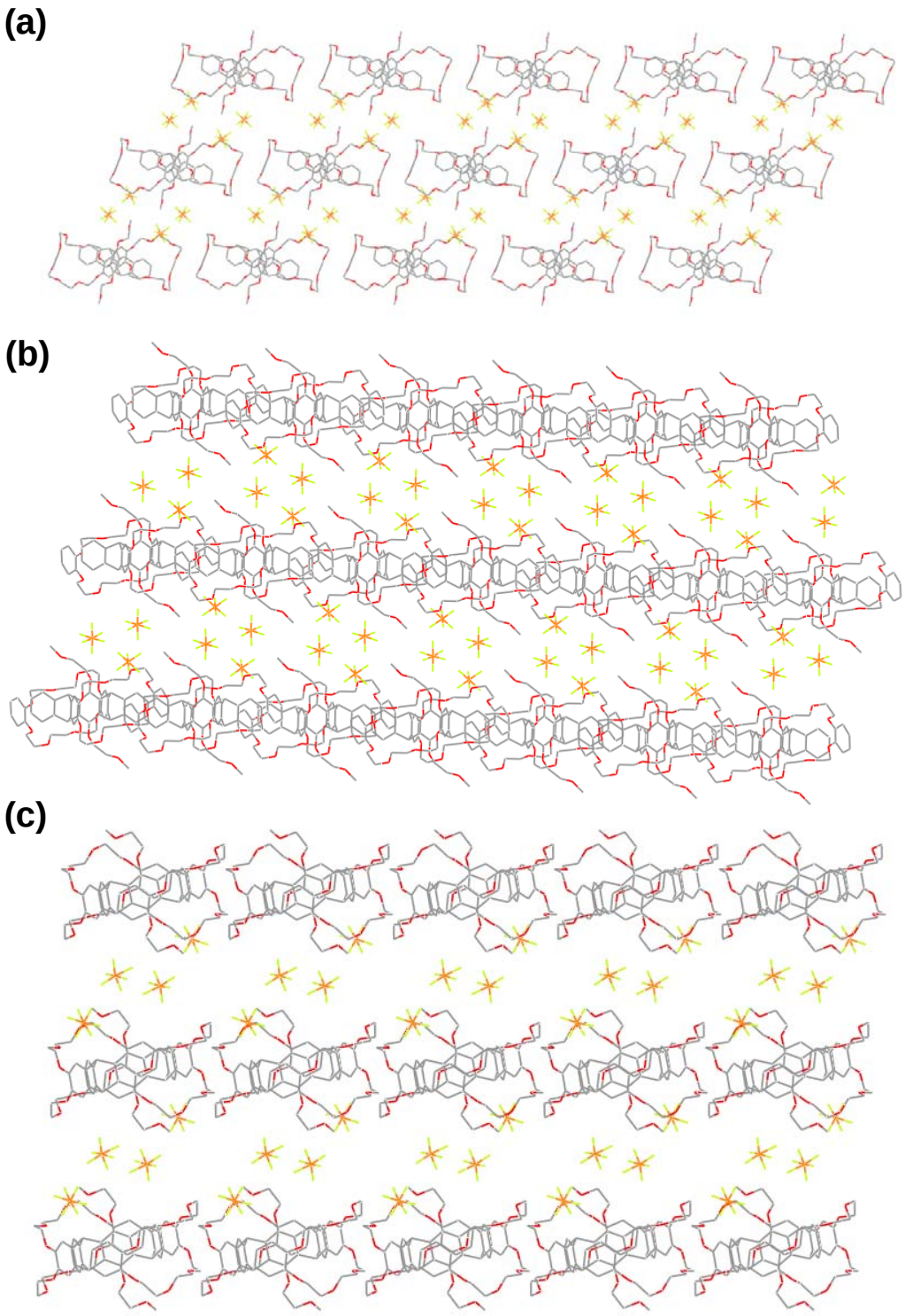

Fig. S77 Packing of the complex (a) **1**•**2**$_2$ viewed along the *a* axis, (b) **1**•**8**$_2$ viewed along the *b* axis and (c) **1**•**11**$_2$ viewed along the *c* axis. Solvent molecules, guest molecules, and hydrogen atoms were omitted for clarity.